AD A107849

AUSTRALIA

DEPARTMENT OF DEFENCE

DEFENCE SCIENCE AND TECHNOLOGY ORGANISATION

AERONAUTICAL RESEARCH LABORATORIES

MELBOURNE, VICTORIA

MECHANICAL ENGINEERING NOTE 385

A PREDICTION METHOD FOR TURBULENT BOUNDARY LAYERS IN ADVERSE PRESSURE GRADIENTS

by

W. H. SCHOFIELD

NOV 3 0 1981

A

Approved for Public Release.

AR-002-257

DEPARTMENT OF DEFENCE
DEFENCE SCIENCE AND TECHNOLOGY ORGANISATION
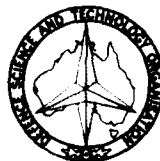AERONAUTICAL RESEARCH LABORATORIES

MECHANICAL ENGINEERING NOTE 385

A PREDICTION METHOD FOR TURBULENT BOUNDARY LAYERS IN ADVERSE PRESSURE GRADIENTS

by

W. H. SCHOFIELD

SUMMARY

A prediction method for turbulent boundary layers in moderate to strong adverse pressure gradients is presented. The closure hypothesis for the method is the universal velocity defect law of Schofield and Perry (1972) which restricts the method to the prediction of layers in moderate to strong adverse pressure gradient. The method is tested against nine experimentally measured boundary layers. Predictions for velocity profile shape, boundary layer thicknesses and velocity scale ratio were generally in good agreement with the experimental measurements and were superior to those given by other prediction methods. Unlike other methods the present method also gives reasonably accurate predictions for the shear stress profile of a layer. The analysis presented here is compared with previous work and helps to resolve some disagreements discerned in the literature.

DOCUMENT CONTROL DATA SHEET

Security classification of this page: Unclassified

1. Document Numbers
  (a) AR Number:
    AR-002-257
  (b) Document Series and Number:
    Mechanical Engineering Note 385
  (c) Report Number:
    ARL-Mech-Eng-Note-385
	2. Security Classification
	  (a) Complete document:
	    Unclassified
	  (b) Title in isolation:
	    Unclassified
	  (c) Summary in isolation:
	    Unclassified

3. Title: A PREDICTION METHOD FOR TURBULENT BOUNDARY LAYERS
IN ADVERSE PRESSURE GRADIENTS

4. Personal Author(s): Schofield, W. H.	5. Document Date: February, 1981
	6. Type of Report and Period Covered:

7. Corporate Author(s):
Aeronautical Research Laboratories
	8. Reference Numbers
	  (a) Task:
	    DST 80/135

9. Cost Code: 42 7404	(b) Sponsoring Agency: DST 0
10. Imprint: Aeronautical Research Laboratories, Melbourne	11. Computer Program(s) (Title(s) and language(s)):

12. Release Limitations (of the document)   Approved for public release

12.0. Overseas:	N.O.	P.R.	1	A	B	C	D	E	

13. Announcement Limitations (of the information on this page):
No Limitations

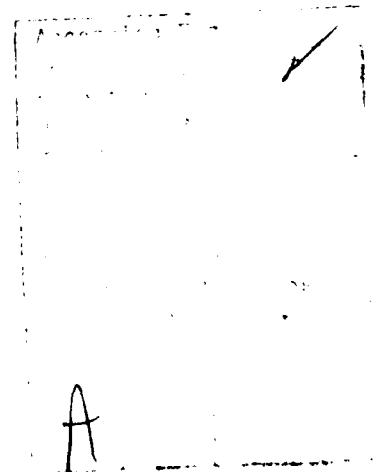| 14. Descriptors:
  Turbulent boundary layer   Boundary layer
  Equilibrium flow   Boundary layer flow
  Prediction analysis techniques Pressure gradients
  Numerical analysis
	15. Cosati Codes:
	2004
	1407

16.
ABSTRACT

A prediction method for turbulent boundary layers in moderate to strong adverse pressure gradients is presented. The closure hypothesis for the method is the universal velocity defect law of Schofield and Perry (1972) which restricts the method to the prediction of layers in moderate to strong adverse pressure gradient. The method is tested against nine experimentally measured boundary layers. Predictions for velocity profile shape, boundary layer thicknesses and velocity scale ratio were generally in good agreement with the experimental measurements and were superior to those given by other prediction methods. Unlike other methods the present method also gives reasonably accurate predictions for the shear stress profile of a layer. The analysis presented here is compared with previous work and helps to resolve some disagreements discerned in the literature.

CONTENTS

NOTATION

a, b, c	constants
B	integral layer thickness ($= 2 \cdot 86\, \delta^*\, U_1/U_s$)
c'_f	skin friction coefficient ($= \tau_0/\frac{1}{2}\rho U_1^2$)
e_1, e_2, e_3, e_4, e_5	constants
f	function of η defined by equation (1)
H	boundary layer shape factor ($= \delta^*/\theta$)
$I_1(\eta)$	$\displaystyle\int_\mu^\eta f\,d\eta$
$I_2(\eta)$	$\displaystyle\int_\mu^\eta f^2\,d\eta$
I_μ	$\displaystyle\int_0^\mu f\,d\eta$
L	distance from wall to τ_m
m	exponent of free stream velocity variation
Re_x	Reynolds number based on development distance x
u	mean velocity in x direction
U_1	free stream velocity
u_0	generalized velocity scale
u_τ	friction velocity ($= (\tau_0/\rho)^{1/2}$)
U_s	velocity scale for Schofield and Perry defect law
U_m	$(\tau_m/\rho)^{1/2}$
x	distance in major flow direction
x_0	effective original of equilibrium layer
X	$(x - x_0)$
y	distance normal to wall
y_c	position of junction between Schofield and Perry defect law and logarithmic law
δ	boundary layer total thickness
δ^*	boundary layer displacement thickness
θ	boundary layer momentum thickness
μ	distance from wall at which $f(\eta)$ accurately describes the mean velocity
ν	kinematic viscosity
η	y/B

$\tau(\eta)$	shear stress
τ_0	wall shear stress
τ_m	maximum shear stress through the layer.

Subscripts

a	actual value
p	predicted value
1	value for type 1 solution
2	value for type 2 solution
I	initial value.

1. INTRODUCTION

The aim of boundary layer research is to provide sufficient understanding of boundary layer behaviour to enable the development of any boundary layer on any surface in any pressure gradient to be accurately predicted. It will be many years before this aim is realized. For quite some time it has been possible to accurately predict simple flows such as flow over a flat plate or within a circular pipe. Recent work has been directed towards predicting boundary layer development in pressure gradients, particularly adverse pressure gradients. The emphasis on adverse pressure gradient layers arises from their practical importance as these are the layers that separate and thus limit the performance of aerodynamic devices. The Stanford conference on computation of turbulent boundary layers (Kline *et al.* (1968), Coles and Hirst (1968)) required authors to predict all mean flow features of a series of boundary layers from a knowledge of the external pressure gradient applied to the layer and details of the boundary layer at the start of the pressure gradient, i.e. the boundary and initial conditions of the layer. The evaluation committee of the conference considered that comparisons between predicted and actual mean velocity profiles, although important, were not as searching as comparisons involving skin friction coefficients (c_f'), form factors (H), and momentum thickness Reynolds numbers. Both mean profile comparisons and parameter comparisons are used here to test the prediction method presented.

To develop this prediction method the simplest case of adverse pressure gradient boundary layers, equilibrium layers, is analysed here. Townsend (1976) defines an equilibrium layer as one in which "the conditions at the initiation of the flow are largely irrelevant and so the flow depends on one or two simple parameters and is geometrically similar at all stations". The "simple parameters" are usually a velocity and length scale for the layer and the geometrical similarity of the layer means that the equation of motion for the layer does not involve the development distance, x. These requirements simplify the computational work although the remaining task is still quite complex.

The prediction method presented here does not need to be restricted to equilibrium flow. By using the concept of "moving equilibrium" the method can be used to predict the development of non-equilibrium layers in which the boundary conditions of the flow vary only slowly with x. The concept of moving equilibrium assumes that these layers make small continuous adjustments to changes in boundary conditions such that they can always be considered to be (locally) in a state of equilibrium. It is a concept used by many existing prediction methods, see Yaglom (1979). The assumption of moving equilibrium does mean that the prediction method cannot be applied to flows in which the boundary conditions change impulsively or even very rapidly.

2. PREVIOUS WORK

The boundary layer prediction method presented here is based on the author's (Schofield (1980)) theoretical analysis of equilibrium boundary layers. This analysis uses the Schofield and Perry (1972) defect law, viz

$$\frac{U_1 - u}{U_s} = 1 - 0 \cdot 4\,(y/B)^{1\cdot 2} - 0 \cdot 6 \sin\left(\frac{\pi}{2} y/B\right) = f(\eta) \tag{1}$$

U_s is a "slip" velocity determined by extrapolating equation (1) to the wall. It is related to the maximum shear stress magnitude (τ_m) and position (L) and the integral thickness of the layer (B) by the relation;

$$U_s^2 = 64 \frac{\tau_m}{\rho} \frac{B}{L} = 64 \, U_m^2 \frac{B}{L} \tag{2}$$

1

see Perry and Schofield (1973). Equation 1 gives an accurate description of, at least, the outer 95% of the mean profile of boundary layers in moderate to strong adverse pressure gradients.

The Schofield analysis of equilibrium layers differs from previous analyses in that the mean profile description, equation (1), is invariant with pressure gradient and hence gives mathematical closure without further hypothesis. As equation (1) is only valid in layers in which $\tau_m/\tau_0 > 3/2$, i.e. layers in moderate to strong adverse pressure gradients (see Schofield and Perry (1972)), the mathematical closure that the equation gives is similarly restricted. Other calculation methods require a hypothesis, in addition to the mean velocity description, in order to get mathematical closure. These hypotheses are usually approximate to some degree and often have to be modified for different classes of boundary layer. Predictions resulting from such hypotheses must be approximate.

The Schofield (1980) analysis of equilibrium flow gave three conditions for the existence of an equilibrium layer, viz;

$$U_1 = a (x - x_0)^m \tag{3}$$

$$U_s = b (x - x_0)^m \tag{4}$$

$$B = c (x - x_0) \tag{5}$$

where a, b, c, x_0 and m are constants[1]. For such equilibrium layers Schofield was able to define limits within which they must exist. These limits are shown in Figure 1 which is reproduced from Schofield (1980). The horizontal axis (m) is the exponent of the free stream velocity variation which is the major boundary condition of the flow. Another boundary condition is surface roughness. The vertical axis is the velocity ratio U_1/U_s, which is constant in an equilibrium layer and is the major initial condition of the flow. Another initial condition is the initial layer thickness. A degree of validation for the theory was provided by the fact that all experimentally observed equilibrium layers were shown to fall within the theoretical limits as shown in Figure 1.

A review of the literature on equilibrium layers (Schofield (1980)) showed that there was significant disagreement between authors on:

(i) the limits for m within which equilibrium layers exist,

(ii) how many different equilibrium layers can exist for a given set of initial and boundary conditions,

(iii) the relationship (if any) between m and the velocity ratio U_1/U_s.

As a result of the theoretical analysis some progress was made in answering these questions and the development of the present prediction method makes some further progress.

3. CALCULATION PROCEDURE

3.1 Assumed Mean Profile

It is assumed that all mean velocity profiles of two-dimensional turbulent boundary layers developing in moderate to strong adverse pressure gradients can be described by the following system of equations;

(i) for the viscous sublayer which extends from $y = 0$ to $y = 10\nu/u_\tau$,

$$u(y) = \frac{y u_\tau^2}{\nu} \tag{6},$$

(ii) for the logarithmic law of the wall, which extends from $y = 10\nu/u_\tau$ to its tangential junction with the velocity defect law at $y = y_c$ (Shown by Perry and Schofield (1973) to be

given by $$y_c = 37 \cdot 1 \frac{u_\tau^2}{U_s^2} B \tag{7}$$

[1] For application to the prediction of layers in moving equilibrium, these constants are replaced by slowly varying functions of x.

$$u(y) = 2 \cdot 44 \, u_\tau \log_e (y u_\tau / \nu) + 5 \cdot 0 \, u_\tau \qquad (8),$$

(iii) for the outer flow extending from $y = y_c$ to $y = B$, the Schofield and Perry defect law, equation (1), rewritten as;

$$u(y) = U_1 - U_s + 0 \cdot 4 \, U_s (y/B)^{1 \cdot 2} + 0 \cdot 6 \, U_s \sin\left(\frac{\pi}{2} y/B\right) \qquad (9)$$

where $B = 2 \cdot 86 \, \delta^* \, U_1/U_s$ $\qquad (10),$

see Schofield and Perry (1972).

3.2 System of Equations

To specify or predict any mean profile $(u(y))$ described by the three equations above (equations (6), (8) and (9)) values for u_τ, U_s and B are required. These values are found by the solution of three simultaneous equations. The first equation has already been introduced and is the relation between the equilibrium layer's thickness and development distance,

$$B = c \, (x - x_0) \qquad (5).$$

The second equation is derived from the integrated equation of motion for an equilibrium layer which was given by Schofield (1980) as,

$$\frac{\tau(\eta)}{\frac{1}{2}\rho U_1^2} = c_f' - 0 \cdot 04 \, mc - \frac{2cb^2}{a^2} \left\{ \frac{a}{b} (3m + 1) I_1(\eta) - (2m + 1) I_2(\eta) \right.$$

$$\left. - \frac{a}{b}(m + 1)(\eta f - \mu f(\mu)) + (m + 1)\left[f I_1(\eta) + f I\mu - f(\mu) I\mu \right] \right\} \qquad (11)$$

where μ, $f(\mu)$, $I\mu$ are constants and $I_1(\eta)$, $I_2(\eta)$, $f I_1(\eta)$ are derived and tabulated in Schofield. The equation used here is the particular case of (11) for $\eta = 1$ which can be written

$$u_\tau^2 = cU_1^2\left[0 \cdot 02 \, m + \frac{U_s}{U_1}(3m + 1) I_1(1) - \frac{U_s^2}{U_1^2}(2m + 1) I_2(1) \right.$$

$$\left. + \frac{U_s}{U_1}(m + 1) \mu f(\mu) - \frac{U_s^2}{U_1^2}(m + 1) f(\mu) I\mu \right] \qquad (12)$$

because $f(1) = 0$ and $\tau(1) = 0$.

The third equation is derived from the observation of Perry and Schofield (1973) that in adverse pressure gradient boundary layers the inner (logarithmic) law tangentially joins the outer (defect) law with little to no blending or crossover region. If this is so, then the expressions for the velocity at $y = y_c$ given by the two laws will be equivalent and equating them will yield an accurate relation between variables. Near $y = y_c$, Perry and Schofield (1973) show that the outer defect law, equation (9) is most accurately described by

$$u(y) = 0 \cdot 47 \, U_1 \left(\frac{U_s}{U_1}\right)^{3/2} \left(\frac{y}{\delta^*}\right)^{1/2} + U_1 - U_s.$$

Substitution of $y = y_c = 37 \cdot 1 \, u_\tau^2/U_s^2 \, B$ into this and into equation (8) (the logarithmic law) leads to

$$U_s = U_1 - 8 \cdot 98 \, u_\tau - 2 \cdot 44 \, u_\tau \left[\log\left(\frac{u_\tau}{U_s}\right)^2 + \log\left(\frac{u_\tau}{U_1}\right) + \log\left(\frac{BU_1}{\nu}\right) \right] \qquad (13)$$

Equation (13) is the third equation required for the calculation method.

3

3.3 Profile Prediction Procedure

The calculation procedure is commenced by matching the initial and boundary conditions to the assumption of equilibrium flow. This is to determine values for the characteristic constants for the flow (m, c, x_0) which are invariant for an equilibrium layer.

To begin, an estimate of m is obtained from the free stream velocity data using equation (3) rewritten in the form

$$\log U_1 = m \log (x - x_0) + \log a \tag{14}.$$

The free stream velocity data, $U_1(x)$, is fitted to equation (14) using linear regression thus determining a value for m. For this initial iteration x_0, the effective origin of the equilibrium layer, is taken as zero. Substituting this estimate for m into equation (12), gives a relationship between u_τ, U_s and c for the equilibrium layer. From the initial mean velocity profile we can determine both u_τ (using the method of Clauser (1954)) and U_s (using the method of Perry and Schofield (1973)). Thus we may solve the equation for c, the (constant) growth rate of the boundary layer. As the value of m that has been used is only an estimate this value of c is also an estimate. Iteration starts by obtaining an estimate for x_0 using equation (5) in which the initial layer thickness and this initial estimate for c are substituted, viz:

$$B_I = c' (x_I - x_0)$$

where subscript I refers to initial conditions and c' is the first estimate for c. The resulting estimate of x_0 is used in equation (14) to give a new, more accurate, estimate of m and the whole process is repeated until the values of m, c and x_0 are stable.

Having established these constants for the layer, values of the parameters u_τ, U_s and B for profiles downstream of the initial profile are calculated in the following manner. The value of B, the layer thickness, can be directly determined from equation (5) as c and x_0 are known. The velocities u_τ and U_s are then determined by simultaneously solving equations (12) and (13). The solution area of these two equations is illustrated in Figure 2 and is further discussed in Section 5. With values for B, u_τ, U_s at every station the mean velocity profiles can be predicted using equations (6), (8) and (9). From these profiles other integral layer thicknesses (θ, δ^*) can be calculated. Finally predictions of shear stress profile can be made using equation (11) with the appropriate predicted values for c_f' ($= 2u_\tau^2 U_1$) and $a b$ ($= U_1 U_s$).

3.4 Comparison of Predictions with Data

The above prediction method was tested on the nine equilibrium layers detailed in Schofield (1980). The results are shown in Figures 3 to 6.

In Figure 3 the predicted and measured values of the parameters m, c and x_0 are compared. On each graph the straight line represents perfect agreement between measurement and prediction. In general the agreement is good, however three of the results for x_0 appear to fall well off the line. As these data are dimensional it is difficult to evaluate how significant the error is. However it can be said that these discrepancies have little effect on the predictions as the same three layers are among the better predicted layers presented here.

Predicted mean velocity profiles are compared with measurement in Figure 4. In these graphs distance from the wall has not been non-dimensionalized in order that the predicted and actual total layer thicknesses can be compared as well as the shape of the mean velocity profiles. Of the nine layers considered, four of the predictions (for layers I, IV, VI, VIII) could be described as excellent for both profile shape and layer total thickness. Of the remaining five layers, predictions in four cases (for layers II, III, VII, IX) could be described as fair to good while in the remaining case (layer V) the prediction of layer total thickness was good but the prediction of profile shape was poor.

In general the above picture is reflected in the predictions of the velocity ratios (U_1/U_s, u_τ/U_1) and integral thicknesses (θ, $H = \delta^*/\theta$) shown in Figure 5. The agreements shown are at least as good as the best predictions given by the methods presented at the Stanford conference (see Kline et al. (1968) p. 533 to p. 569). in particular the predictions for layers VII and IX, the separating layers of Stratford (1959). appear to be substantially better predicted by the present method than by any of the methods presented at the Stanford conference.

4

There are discernible differences between the comparisons in Figure 4 and those in Figure 5. For instance the prediction of the velocity ratios for layer I could only be described as good whereas the mean profile predictions are excellent. On the other hand predictions of velocity ratios and integral thicknesses for layer V seem superior to the corresponding predictions of mean profile shape. Thus although the evaluation committee at the Stanford conference considered comparisons such as those shown in Figure 5 to be the most searching test of a prediction method, the results presented here show that the two comparisons appear to test different aspects of a prediction method.

Figure 6 compares measured shear stress data across the boundary layer with predicted shear stress profiles calculated using predicted values for the parameters m, c, U_1/U_s ($= a/b$) and c_f' ($= 2u_\tau^2/U_1^2$). On the same figures, predicted shear stress profiles calculated using actual values of the parameters m, c, U_1/U_s, c_f' are also shown. As is to be expected these latter profiles show better agreement with the measured shear stress data than the profiles calculated using predicted values for the parameters. Differences are, however not large and thus this prediction method provides a useful estimate of shear stress throughout the layer. This is not provided by any other prediction method known to the author. Reynolds shear stress is directly related to the (turbulent) transport of momentum across a sheared layer (Hinze (1959) p. 278) and this transport rate is closely connected to mass and heat transport across the layer (see Hinze (1959), Schofield and Keeble (1975)). Consequently the prediction method presented here would be useful in estimating local or overall rates for these transport mechanisms in heat and mass transfer problems.

4. ASPECTS OF THE SOLUTIONS

The prediction method presented here requires the simultaneous solution of equations (12) and (13) to find values for u_τ, U_s for each profile. For any particular profile in a given boundary layer equation (12) has the form

$$u_\tau^2 = c\,(e_1\,U_s^2 + e_2\,U_s + e_3) \tag{15}$$

where $e_1, \ldots, e_n$ are constants for a particular profile. Equation (13),

$$U_s = U_1 - 36\cdot05\,u_\tau - 2\cdot44\,u_\tau\,\log_e\left(\frac{Bu_\tau^3}{U_s^2}\right) \tag{13}$$

is to a first approximation

$$U_s \simeq e_4 + e_5\,u_\tau \tag{16}$$

i.e., a linear relationship. The simultaneous solution of these two equations, illustrated in Figure 2, give two solutions:

a type 1 solution—moderate velocity defect with a large wall stress (moderate U_s and high u_τ),

a type 2 solution—very large velocity defect with a much lower wall shear stress (high U_s and low u_τ).

The intersections between the two solution curves can be divided into three different cases. The first case (curve a on Fig. 2) gives two solutions with positive wall shear, i.e. positive values of u_τ. The second case (curve c on Fig. 2) gives one solution with positive wall shear and one solution with negative wall shear. As negative wall shear implies reversed flow near the wall it is a solution that is outside one of the assumptions of the analysis. This solution cannot therefore be regarded as a legitimate equilibrium layer predicted by the analysis. For this case therefore the analysis predicts only one equilibrium layer. The third case (curve d on Fig. 2) gives two solutions with negative wall shear and thus in this case the analysis predicts no (attached) equilibrium layers.

For the first case, a layer with a set of boundary and initial conditions that gives two solutions with positive values of u_τ, the correct solution is simply chosen as the one in which the predicted values of U_1/U_s and u_τ/U_1 agree with the given initial conditions of the layer. For the layers analysed in this report, layers II, IV, VI, VIII have type 1 solutions while layers I, III,

5

V, VII, IX have type 2 solutions. Townsend's (1960, 1976) analysis also predicts two possible equilibrium layers for a single set of conditions. His analysis of layer II (of this report) shows it to be a type 1 solution (moderate U_s, high u_τ) which is in agreement with the present analysis. However Townsend's theory puts layer III of this report in "an area of ambiguous development and its observed development is not described by this theory", Townsend (1960). Layer III is well described by the present theory and is a type 2 solution. Townsend (1976, p. 276) also gives $m = 0.25$ as the lower limit above which there is only one solution with positive u_τ, i.e. curve (b) on Figure 2 relates to a layer where $m = 0.25$. The present analysis however gives values of m for layers II, VII and IX which are substantially greater than -0.25 and yet have two solutions that have positive values of u_τ. Another estimate for the value of m above which only one attached solution can exist can be obtained from the present analysis. The limiting condition is defined by $u_\tau = 0$ which when substituted into equation (13) gives

$$ U_s - U_1 = 36 \cdot 05(0) - 2 \cdot 44 \, (0) \log_e \left(\frac{B(0)^3}{U_s^2} \right) . $$

As the last term in this expression is indeterminate at $u_\tau = 0$ it is evaluated by l'Hôpital's rule. The indeterminate portion of the term is $u_\tau \log_e u_\tau^3$ which can be rewritten $\log_e u_\tau^3 / 1 / u_\tau$. Differentiation gives

$$ \frac{(d(\log_e u_\tau^3) / du_\tau^3) du_\tau^3 / du_\tau}{d(1/u_\tau) / du_\tau} = \frac{3u_\tau^2 u_\tau^3}{1/u_\tau^2} = 3u_\tau . $$

Thus as $u_\tau \to 0$, $u_\tau \log_e u^3_\tau \to 0$ and hence equation (13) at $u_\tau = 0$ reduces to

$$ U_s = U_1 \tag{17}. $$

The theory of Perry and Schofield (1973) shows that for a layer in which $U_s = U_1$ the junction between the half power and logarithmic law is on the wall, i.e. there is no logarithmic law. In fact this is not possible because of the laminar sublayer immediately adjacent to the wall. The existence of the laminar sublayer has not been included in the above analysis and thus equation (17) is an approximation to the limiting condition. However as the sublayer is very thin the approximation is a fairly good one. Substitution of (17) into the other solution equation (equation (12)) gives

$$ 0 \cdot 02 \, m - (3m-1) I_1(1) - (2m-1) I_2(1) - (m-1) \mu f'(\mu) - (m-1) f(\mu) I_\mu = 0, $$

and substitution of values for $I_1(1)$, $I_2(1)$, $\mu f'(\mu)$, $f(\mu) I_\mu$ from Schofield (1980) gives an equation in m which has as its solution

$$ m = 0 \cdot 23 . $$

This limit is higher than Townsend's value but is in accord with the present results. All layers in which the predicted value of m was less than $0 \cdot 23$ had two attached solutions and the only layer where $m_p > 0 \cdot 23$ had only one attached solution (see table 1).

Bradshaw (1966) disputed Townsend's result that two equilibrium layers were possible for a given set of conditions. Bradshaw attributed the result to Townsend's assumption of a smooth junction between the two (approximate) expressions for the mean velocity in the inner and outer regions. Bradshaw stated that although both solutions were good approximations far from the join the assumption of a smooth join is unlikely to be accurate for layers with large velocity defects. The present analysis makes the same assumption that was made by Townsend. However in this case there is good evidence, in Perry and Schofield (1973), that the two expressions for the mean velocity used here do join tangentially with little to no blending region. This work does not therefore support the argument of Bradshaw (1966) nor the conclusion of Mellor and Gibson (1966) of a single series of equilibrium layers terminating at $m = 0 \cdot 23$ (see Schofield (1980) for details). It seems likely that the approximate analysis of Mellor and Gibson only yields the low wall shear or type 2 solution which does not exist for $m > 0 \cdot 23$.

The layers predicted by the present analysis are plotted on m, U_1 / U_s co-ordinates in Figure 7. All predicted layers are within the limits for equilibrium layers delineated by Schofield (1980) and are close to the positions of the measured layers. Also plotted on the figure are the alternative second solutions given by the method. These second solutions are well removed

from the position of the measured layers but are still within the limits for equilibrium layers. The one exception to this is the second solution for layer IX which falls well outside the limits for equilibrium layers with U_1/U_s 5 for m_p $0\cdot231$. Such a layer with a velocity ratio of 5 would have an extremely small velocity defect and have a very high wall shear which are characteristics of layers in strong *favourable* pressure gradients. Such a layer would not be described by the Schofield and Perry (1972) defect law and this is confirmed by the position of the solution on m, U_1/U_s co-ordinates which puts it well outside the region where the Schofield and Perry defect law is valid. This second solution is thus outside one of the assumptions of the analysis and therefore cannot be regarded as a legitimate equilibrium layer predicted by the analysis.

Finally we can show how some calculations of Head (1976) can be explained in terms of the present analysis. Head's calculations for three different equilibrium layers suggested that;

(i) for m $-0\cdot35$ no equilibrium layer was possible.

(ii) for m $-0\cdot15$ only one equilibrium layer was possible irrespective of the initial conditions,

(iii) for m $-0\cdot255$ a range of equilibrium layers is possible. The particular equilibrium layer that develops depends on the initial conditions of the layer. In particular as the initial value of $U_1\,\theta'\nu$ is increased the equilibrium layer generated approaches separation and eventually separates.

The first conclusion is in agreement with the limits shown in Figures 1 and 7 and has been previously discussed in Schofield (1980).

The second conclusion was in fact only strongly suggested by Head's calculations. The calculations consisted of a series of predictions for layer development in a set pressure gradient ($m = -0\cdot15$) and for a given initial boundary layer shape (H constant) but with differing initial thicknesses (θ_I). The calculations showed the several boundary layer developments apparently converging on a single equilibrium layer. However the calculations were not continued far enough to prove the point. The present theory has shown that for $m = -0\cdot15$ only one (attached) solution for any given initial boundary layer shape (U_1/U_s) can be expected. But Head investigated changes in the other initial condition, the initial layer thickness (B_I). Changes in B_I cause, through the initial matching procedure, changes in m, c, and x_0 which entail changes in layer thickness at all downstream stations. The effect is to magnify the parabola, equation 12 on Figure 2, but to lower the position of the (nearly) straight line, equation 13 on Figure 2. The two effects are to a certain extent self-cancelling but do result in a lower solution position and thus slightly lower values of u_τ and U_s for the equilibrium layer. Thus this conclusion of Head appears to be correct to a first approximation only.

Head's third conclusion is that for flows with m $-0\cdot255$ a wide range of equilibrium layers exist depending on the initial thickness. An additional conclusion is that for large initial thicknesses the layer will separate before equilibrium conditions are established. As $m = -0\cdot255$ is below the limit of $-0\cdot23$ two solutions for each set of initial and boundary conditions would be expected. Apparently Head's calculation method gives only one of these solutions. As discussed above, the solutions will change as B_I is increased and the trend will be for the wall shear stress to approach zero. Head's calculations predicted separated flow for layer V if the initial layer thickness was twice the actual value. However calculations varying B_I for layer V using the present method did not predict separation even for initial layer thicknesses one hundred times the measured value. Although the predicted wall shear stress was reduced it did not become negative. This is to be expected as the analysis earlier in this section shows that provided the boundary conditions do not change and $m < -0\cdot23$ then, irrespective of the initial conditions, there are two solutions with positive u_τ.

5. CONCLUSIONS

1. A simple prediction method for turbulent boundary layers in moderate to strong adverse pressure gradient can be based on the Schofield and Perry defect law. For equilibrium layers in adverse pressure gradient the prediction method gives;

7

(a) accurate predictions for mean velocity profile shape and total layer thickness,

(b) accurate predictions of momentum thickness, wall shear, velocity scale ratio and form factor,

(c) reasonably accurate predictions for the shearing stress profile across the layer.

2. For a given set of boundary conditions two types of layers can develop; a layer with a moderate mean velocity defect and a large wall shear or a layer with a large mean velocity defect and a small wall shear. Which type of layer develops in practice depends on the velocity ratio of the initial profile.

3. For flows in which the free stream velocity exponent (m) is greater than about -0.23 only the layer with a moderate mean velocity defect can develop. In this case the solution for the layer with large mean velocity defect has a negative wall shear which is outside the bounding assumptions of the analysis and thus is not a legitimate prediction.

4. For a given initial velocity ratio and a given set of boundary conditions, increasing the initial layer thickness decreases the wall shear stress of a layer generated by the flow conditions. However calculations suggest that for realistic increases of initial layer thickness the predicted wall shear stress shows little change.

REFERENCES

Bradshaw, P., (1966)—N.P.L. Aero. Rept. 1184. See also J. Fluid Mech., (1967), Vol. 29, p. 625.

Bradshaw, P., (1967)—N.P.L. Aero. Report. 1219.

Bradshaw, P., and Ferriss, D., (1965)—N.P.L. Aero. Rept. 1145.

Clauser, F. H., (1954)—J. Aero. Sci., Vol. 21, p. 91.

Coles, D. E., and Hirst, E. A. (1968)—AFSOR-IFP-Stanford Conference, Vol. 2.

Head, M. R. (1976)—J. Fluid Mech., Vol. 73, part 1, pp. 1-8.

Hinze, J. O. (1959)—Turbulence, McGraw-Hill.

Kline, S. J., Morkovin, M. V., Sovran, G., and Cockrell, D. J. (1968)—AFOSR-IFP-Stanford Conference, Vol. 1.

Ludwieg, H., and Tillmann, W. (1949)—Ing.-Arch., Vol. 17, p. 288. See also NACA TM 1285 (1950).

McQuaid, J. (1965)—A.R.C. paper 27 287.

Mellor, G. L. (1966)—J. Fluid Mech., Vol. 24, p. 255.

Mellor, G. L., and Gibson, D. M. (1966)—J. Fluid Mech., Vol. 24, p. 225.

Perry, A. E., and Schofield, W. H. (1973)—Phys. of Fluids, Vol. 16, p. 2068.

Reynolds, W. C. (1968)—In Kline et al. (op. cit) p. 1.

Rotta, J. C. (1962)—Prog. in Aero. Sci., Vol. 2, p. 3, Ferri-Pergamon.

Samuel, A. E. (1973)—Ph.D. Thesis, Univ. of Melb.

Schofield, W. H. (1980)—A.R.L., Mech. Eng. Rept. 157.

Schofield, W. H., and Keeble, T. S. (1975)—Trans. A.S.M.E., J. of Fluids Eng., Vol. 97, Ser. 1, No. 3, p. 334.

Schofield, W. H., and Perry, A. E. (1972)—A.R.L. Mech. Eng. Rept. 134.

Stratford, B. S. (1959)—J. Fluid Mech., Vol. 5, p. 1 and p. 17.

Townsend, A. A. (1960)—J. Fluid Mech., Vol. 8, p. 143.

Townsend, A. A. (1961)—J. Fluid Mech., Vol. 12, p. 536.

Townsend, A. A. (1976)—The Structure of Turbulent Shear Flow, 2nd Ed., C.U.P.

Yaglom, A. M. (1979)—Ann. Rev. of Fluid Mech., Vol. 11, p. 505. Eds. Van Dyke, M., Wehausen, J. V., and Lumley, J. L., Annual Reviews Inc.

TABLE 1

Layer I: Ludwieg and Tillmann (1949)

Type 2 Solution

x (m)	B_a (m)	B_p (m)		$u_{\tau a}$ (m/s)	$u_{\tau 1}$ (m/s)	$u_{\tau 2}$ (m/s)
3.332	0.1112	—		0.7283	—	—
3.532	0.1208	0.1222		0.6873	0.6554	0.6554
3.732	0.1304	0.1333		0.6754	0.6824	0.6040
3.932	0.1448	0.1444		0.6225	0.6797	0.5754
4.132	0.1625	0.1554		0.5924	0.6730	0.5520
4.332	0.1772	0.1664		0.5587	0.6625	0.5310

x (m)	$(a/b)_a$	$(a/b)_1$	$(a/b)_2$	$c'_{f_a} \times 10^3$	$c'_{f_1} \times 10^3$	$c'_{f_2} \times 10^3$
3.332	1.818	—	—	1.60	—	—
3.532	1.724	1.619	1.619	1.53	1.39	1.39
3.732	1.667	1.757	1.520	1.52	1.55	1.22
3.932	1.613	1.815	1.487	1.34	1.60	1.15
4.132	1.587	1.859	1.466	1.26	1.63	1.09
4.332	1.515	1.893	1.451	1.17	1.65	1.06

$$m_a = -0.259{,}87 \qquad c_a = 0.067{,}2 \qquad x_{0a} = 1.732 \text{ m}$$
$$m_p = -0.254{,}63 \qquad c_p = 0.055{,}24 \qquad x_{0p} = 1.319 \text{ m}$$

x (m)	δ_a^* (m)	δ_1^* (m)	δ_2^* (m)	θ_a (m)	θ_1 (m)	θ_2 (m)
3.332	0.02138	0.02173	0.02173	0.01432	0.01467	0.01467
3.532	0.02450	0.02652	0.02652	0.01614	0.01710	0.01710
3.732	0.02735	0.02670	0.03078	0.01773	0.01790	0.01918
3.932	0.03139	0.02803	0.03405	0.02005	0.01905	0.02095
4.132	0.03580	0.02949	0.03718	0.02246	0.02023	0.02268
4.332	0.04089	0.03104	0.04023	0.02528	0.02145	0.02439

x (m)	H_a	H_1	H_2
3.332	1.492	1.482	1.482
3.532	1.519	1.551	1.551
3.732	1.542	1.492	1.605
3.932	1.566	1.472	1.625
4.132	1.594	1.458	1.639
4.332	1.618	1.447	1.650

TABLE 1

Layer II: Clauser (1954) Flow 1

Type 1 Solution

x (m)	B_a (m)	B_p (m)		u_{ra} (m/s)	u_{r1} (m/s)	u_{r2} (m/s)
2·1092	0·0679			0·3210	—	—
3·3528	0·1056	0·1222		0·2901	0·2885	0·1129
3·8862	0·1243	0·1455		0·2752	0·2180	0·1031
5·6632	0·1792	0·2232		0·2386	0·2499	0·0826
7·2634	0·2418	0·2931		0·2128	0·2333	0·0721
8·2052	0·2683	0·3342		0·2074	0·2220	0·0668
9·0678	0·2963	0·3719		0·1954	0·2147	0·0632
9·8298	0·3220	0·4052		0·1917	0·2085	0·0603

x (m)	$(a/b)_a$	$(a/b)_1$	$(a/b)_2$	$c_{fa}' \times 10^3$	$c_{f1}' \times 10^3$	$c_{f2}' \times 10^3$
2·1092	1·786			2·10	—	—
3·3528	1·695	1·857	1·062	2·14	2·12	0·32
3·8862	1·724	1·917	1·058	2·08	2·12	0·29
5·6632	1·852	2·059	1·050	1·93	2·12	0·23
7·2634	1·961	2·151	1·046	1·75	2·10	0·20
8·2052	1·887	2·189	1·045	1·83	2·10	0·19
9·0678	2·000	2·222	1·043	1·73	2·09	0·18
9·8298	1·961	2·248	1·043	1·76	2·08	0·17

$$m_a = -0·223,71 \qquad c_a = 0·033,25 \qquad x_{0a} = 0·136 \text{ m}$$
$$m_p = -0·233,76 \qquad c_p = 0·043,69 \qquad x_{0p} = 0·555 \text{ m}$$

x (m)	δ_a^* (m)	δ_1^* (m)	δ_2^* (m)	θ_a (m)	θ_1 (m)	θ_2 (m)
2·1092	0·01378	0·01372	0·01372	0·00871	0·009011	0·00901
3·3528	0·02216	0·02336	0·04066	0·01443	0·01589	0·01852
3·8862	0·02520	0·02699	0·04857	0·01641	0·01858	0·02205
5·6632	0·03384	0·03874	0·07494	0·02286	0·02733	0·03381
7·2634	0·04311	0·04892	0·09871	0·02985	0·03497	0·04441
8·2052	0·05066	0·05495	0·11268	0·03467	0·03947	0·05065
9·0678	0·05388	0·06033	0·12550	0·03734	0·04351	0·05636
9·8298	0·05968	0·06507	0·13682	0·04130	0·04707	0·0614

x (m)	H_a	H_1	H_2
2·1092	1·580	1·523	1·523
3·3528	1·536	1·471	2·195
3·8862	1·535	1·453	2·203
5·6632	1·480	1·417	2·216
7·2634	1·444	1·399	2·223
8·2052	1·461	1·392	2·225
9·0678	1·443	1·387	2·227
9·8298	1·446	1·383	2·228

TABLE 1

Layer III: Clauser (1954) Flow 2

Type 2 Solution

x (m)	B_a (m)	B_p (m)		$u_{\tau a}$ (m/s)	$u_{\tau 1}$ (m/s)	$u_{\tau 2}$ (m/s)
2·286	0·1041	—		0·2028	—	—
2·743	0·1341	0·1314		0·1852	0·2481	0·1788
3·353	0·1571	0·1678		0·1718	0·2374	0·1585
3·862	0·1910	0·1982		0·1557	0·2310	0·1473
4·929	0·2800	0·2619		0·1455	0·2159	0·1294
5·843	0·3459	0·3165		0·1380	0·2045	0·1183
7·291	0·4712	0·4030		0·1256	0·1906	0·1058
8·129	0·5700	0·4530		0·1137	0·1822	0·0995

x (m)	$(a/b)_a$	$(a/b)_1$	$(a/b)_2$	$c_{fa}' \times 10^3$	$c_{f1}' \times 10^3$	$c_{f2}' \times 10^3$
2·286	1·351	—	—	1·30	—	—
2·743	1·282	1·853	1·307	1·20	2·15	1·12
3·353	1·299	1·972	1·276	1·15	2·20	0·98
3·862	1·299	2·051	1·260	1·04	2·21	0·90
4·929	1·333	2·169	1·241	1·05	2·21	0·80
5·843	1·333	2·244	1·231	1·05	2·21	0·74
7·291	1·333	2·338	1·220	0·95	2·19	0·68
8·129	1·333	2·377	1·216	0·85	2·18	0·65

$$m_a = -0.252{,}66 \qquad c_a = 0.033{,}25 \qquad x_{0a} = 1.242 \text{ m}$$
$$m_p = -0.247{,}29 \qquad c_p = 0.059{,}72 \qquad x_{0p} = 0.543 \text{ m}$$

x (m)	δ_a^* (m)	δ_1^* (m)	δ_2^* (m)	θ_a (m)	θ_1 (m)	θ_2 (m)
2·286	0·02767	0·02703	0·02703	0·01547	0·01557	0·01557
2·743	0·03530	0·02518	0·03526	0·01920	0·01709	0·01984
3·353	0·04339	0·03037	0·04609	0·02413	0·02108	0·02548
3·862	0·05143	0·03461	0·05513	0·02868	0·02433	0·03018
4·929	0·07247	0·04353	0·07400	0·04128	0·03110	0·04000
5·843	0·09195	0·05110	0·09017	0·05207	0·03680	0·04840
7·291	0·1236	0·06285	0·11584	0·07036	0·04573	0·06169
8·129	0·15148	0·06969	0·13068	0·08618	0·05089	0·06939

x (m)	H_a	H_1	H_2
2·286	1·788	1·736	1·736
2·743	1·838	1·473	1·777
3·353	1·798	1·441	1·808
3·862	1·794	1·422	1·827
4·929	1·755	1·399	1·850
5·843	1·766	1·387	1·863
7·291	1·757	1·374	1·878
8·129	1·758	1·369	1·883

TABLE 1

Layer IV: Bradshaw (1966) "a $= -0.15$"

Type 1 Solution

x (m)	B_a (m)	B_p (m)		$u_{\tau a}$ (m/s)	$u_{\tau 1}$ (m/s)	$u_{\tau 2}$ (m/s)
0·6096	0·02702	—		1·4628	—	—
1·2192	0·04681	0·0441		1·2781	1·30151	< 0
1·6764	0·06072	0·05691		1·1992	1·2338	< 0
2·1336	0·07470	0·0697		1·1120	1·1815	< 0
					.	
x (m)	$(a/b)_a$	$(a/b)_1$		$c_{fa}' \times 10^3$	$c_{f1}' \times 10^3$	$c_{f2}' \times 10^3$
0·6096	2·000	—		2·24	—	—
1·2192	2·0833	2·145		2·11	2·18	< 0
1·6764	2·0833	2·224		2·03	2·15	< 0
2·1336	2·0833	2·288		1·88	2·12	< 0

$$m_a = -0.212,89 \qquad c_a = 0.031,254 \qquad x_{0a} = -0.264 \text{ m}$$
$$m_p = -0.197,47 \qquad c_p = 0.028,021 \qquad x_{0p} = -0.355 \text{ m}$$

x (m)	δ_a^* (m)	δ_1^* (m)	θ_a (m)	θ_1 (m)	H_a	H_1
0·6096	0·004724	0·004826	0·003327	0·003365	1·426	1·434
1·2192	0·007856	0·007396	0·005664	0·005272	1·387	1·403
1·6764	0·010191	0·009241	0·007315	0·006656	1·391	1·388
2·1336	0·012537	0·011043	0·008966	0·008013	1·399	1·378

TABLE 1

Layer V: Bradshaw and Ferriss (1965) "a $= -0\cdot255$"

Type 2 Solution

x (m)	B_a (m)	B_p (m)		u_{ra} (m/s)	u_{r1} (m/s)	u_{r2} (m/s)
0·5843	0·0349	—		1·1204	—	· ~
1·1940	0·0750	0·0714		0·8904	1·1115	0·7157
1·6510	0·0979	0·0988		0·7993	1·0226	0·6206
2·108	0·1275	0·1262		0·7430	0·9551	0·5576

x (m)	$(a/b)_a$	$(a/b)_1$	$(a/b)_2$	$c_{fa}' \times 10^3$	$c_{f1}' \times 10^3$	$c_{f2}' \times 10^3$
0·5843	1·4706	—	—	1·45	—	—
1·1940	1·5625	2·177	1·30	1·32	2·06	0·85
1·6510	1·6129	2·310	1·28	1·25	2·05	0·75
2·108	1·6129	2·406	1·27	1·23	2·03	0·70

$$m_a = -0\cdot256{,}25 \qquad c_a = 0\cdot0599 \qquad x_{0a} = -0\cdot015 \text{ m}$$
$$m_p = -0\cdot250{,}67 \qquad c_p = 0\cdot0598{,}80 \qquad x_{0p} = 0\cdot0013 \text{ m}$$

x (m)	δ_a^* (m)	δ_1^* (m)	δ_2^* (m)	θ_a (m)	θ_1 (m)	θ_2 (m)
0·5843	0·00830	0·00830	0·00830	0·00504	0·005087	0·005087
1·1940	0·01678	0·1178	0·01930	0·01054	0·008457	0·010804
1·6510	0·02122	0·01549	0·02713	0·01361	0·011283	0·015003
2·108	0·02766	0·01912	0·03499	0·01763	0·014049	0·019197

x (m)	H_a	H_1	H_2
0·5843	1·654	1·632	1·632
1·1940	1·591	1·393	1·786
1·6510	1·558	1·373	1·809
2·108	1·568	1·361	1·822

TABLE 1

Layer VI: Bradshaw (1967) "Flow C"

Type 1 Solution

x (m)	B_a (m)	B_p (m)		$u_{\tau a}$ (m/s)	$u_{\tau 1}$ (m/s)	$u_{\tau 2}$ (m/s)
1·0668	0·04593	—		1·0323	—	—
1·2192	0·05118	0·05279		0·9795	0·9886	0·5767
1·5240	0·06554	0·06651		0·8905	0·9427	0·5143
1·8288	0·07485	0·08022		0·8162	0·9031	0·4696
2·1336	0·08715	0·09394		0·7681	0·8682	0·4352

x (m)	$(a/b)_a$	$(a/b)_1$	$(a/b)_2$	$c_{fa}' \times 10^3$	$c_{f1}' \times 10^3$	$c_{f2}' \times 10^3$
1·0668	1·9231	—	—	1·87	—	—
1·2192	1·8868	1·795	1·180	1·80	1·83	0·62
1·24	1·7857	1·878	1·166	1·66	1·86	0·55
1·8288	1·7241	1·944	1·158	1·53	1·87	0·51
2·1336	1·7241	1·998	1·151	1·47	1·88	0·47

$$m_a = -0·239,261 \qquad c_a = 0·038,65 \qquad x_{0a} = -0·126 \text{ m}$$
$$m_p = -0·248,11 \qquad c_p = 0·045,00 \qquad x_{0p} = +0·046 \text{ m}$$

x (m)	δ_a^* (m)	δ_1^* (m)	δ_2^* (m)	θ_a (m)	θ_1 (m)	θ_2 (m)
1·0668	0·00835	0·00865	0·00865	0·00577	0·00588	0·00588
1·2192	0·00948	0·01038	0·01568	0·00650	0·00700	0·00811
1·5240	0·01237	0·01253	0·01998	0·00828	0·00860	0·01023
1·8288	0·01518	0·01463	0·02429	0·00998	0·01017	0·01234
2·1336	0·01767	0·01670	0·02860	0·011557	0·01172	0·01445

x (m)	H_a	H_1	H_2
1·0668	1·449	1·472	1·472
1·2192	1·460	1·484	1·933
1·5240	1·495	1·457	1·954
1·8288	1·521	1·438	1·969
2·1336	1·530	1·425	1·980

TABLE 1

Layer VII: Stratford (1959) "Flow 5"

Type 2 Solution

x (m)	B_a (m)	B_p (m)		$u_{\tau a}$ (m/s)	$u_{\tau 1}$ (m/s)	$u_{\tau 2}$ (m/s)
0·926	0·01792	—		0·4048	—	—
1·076	0·03205	0·02788		0·3276	0·5211	0·2863
1·251	0·04121	0·03992		0·3449	0·4933	0·2456
1·622	0·05976	0·06559		0·2945	0·4286	0·1931
1·901	0·08236	0·08484		0·2555	0·3907	0·1689

x (m)	$(a/b)_a$	$(a/b)_1$	$(a/b)_2$	$c_{fa}' \times 10^3$	$c_{f1}' \times 10^3$	$c_{f2}' \times 10^3$
0·926	1·220	—	—	1·42	—	—
1·076	1·205	2·094	1·151	1·19	2·37	0·91
1·251	1·316	2·284	1·132	1·45	2·51	0·74
1·622	1·333	2·507	1·116	1·36	2·56	0·58
1·901	1·299	2·610	1·110	1·21	2·55	0·53

$$m_a = -0.243,13 \qquad c_a = 0.062,88 \qquad x_{0a} = 0.616 \text{ m}$$
$$m_p = -0.239,51 \qquad c_p = 0.069,10 \qquad x_{0p} = 0.673 \text{ m}$$

x (m)	δ_a^* (m)	δ_1^* (m)	δ_2^* (m)	θ_a (m)	θ_1 (m)	θ_2 (m)
0·926	0·00501	0·00503	0·00503	0·00300	0·002668	0·002668
1·076	0·00930	0·00490	0·00858	0·00490	0·003380	0·004247
1·251	0·01095	0·00655	0·01246	0·00610	0·004625	0·006098
1·622	0·01567	0·01007	0·02069	0·00884	0·007248	0·010040
1·901	0·02246	0·01267	0·02688	0·01232	0·009190	0·01300

x (m)	H_a	H_1	H_2
0·926	1·671	1·887	1·887
1·076	1·895	1·451	2·021
1·251	1·795	1·417	2·042
1·622	1·771	1·389	2·061
1·901	1·822	1·379	2·068

TABLE 1

Layer VIII: Samuel (1973)

Type 1 Solution

x (m)	B_a (m)	B_p (m)		$u_{\tau a}$ (m/s)	$u_{\tau 1}$ (m/s)	$u_{\tau 2}$ (m/s)
2·9	0·1022	—		0·6721	—	—
3·38	0·1217	0·1270		0·6050	0·6415	0·4119
x (m)	$(a/b)_a$	$(a/b)_1$	$(a/b)_2$	$c_{fa}' \times 10^3$	$c_{f1}' \times 10^3$	$c_{f2}' \times 10^3$
2·9	1·92	—	—	1·85	—	—
3·38	1·82	1·986	1·27	1·66	1·866	0·77

$$m_a = -0.239,59 \qquad c_a = 0.040,63 \qquad x_{0a} = 0.384,3 \text{ m}$$
$$m_p = -0.248,11 \qquad c_p = 0.051,63 \qquad x_{0p} = 0.920,8 \text{ m}$$

x (m)	$\delta_a{}^*$ (m)	$\delta_1{}^*$ (m)	$\delta_2{}^*$ (m)	θ_a (m)	θ_1 (m)	θ_2 (m)
2·9	—	0·01890	0·01890	—	0·01306	0·01306
3·38	—	0·02270	0·01931	—	0·01590	0·01931
x (m)	H_a	H_1	H_2			
2·9	—	1·447	1·447			
3·38	—	1·4273	1·818			

TABLE 1

Layer IX: Stratford (1959) "Flow 6"

Type 1 Solution

x (m)	B_a (m)	B_p (m)		$u_{\tau a}$ (m/s)	$u_{\tau 1}$ (m/s)	$u_{\tau 2}$ (m/s)
0·926	0·01686	—		0·3337	—	—
1·0763	0·03493	0·03404		0·2134	0·5526	0·1685
1·2506	0·05002	0·05395		0·1932	0·4921	0·1379
1·6221	0·09277	0·09641		0·1308	0·4065	0·1039
1·9007	0·1199	0·12825		0·1165	0·3672	0·0901

x (m)	$(a/b)_a$	$(a/b)_1$	$(a/b)_2$	$c_{fa}' \times 10^3$	$c_{f1}' \times 10^3$	$c_{f2}' \times 10^3$
0·926	1·0640	—	—	0·99	—	—
1·0763	0·9804	4·318	1·032	0·55	3·614	0·34
1·2506	0·9709	4·645	1·029	0·53	3·374	0·27
1·6221	0·9091	5·015	1·026	0·33	3·128	0·20
1·9007	0·8772	5·188	1·025	0·31	3·020	0·18

$$m_a = -0·219,426 \qquad c_a = 0·105,921 \qquad x_{0a} = 0·761,3 \text{ m}$$
$$m_p = -0·231,16 \qquad c_p = 0·114,277 \qquad x_{0p} = 0·778,4 \text{ m}$$

x (m)	$\delta_a{}^*$ (m)	$\delta_1{}^*$ (m)	$\delta_2{}^*$ (m)	θ_a (m)	θ_1 (m)	θ_2 (m)
0·926	0·00554	0·00554	0·00554	0·00307	0·00260	0·00260
1·0763	0·01258	0·005896	0·01227	0·00538	0·00433	0·00484
1·2506	0·01819	0·009221	0·01910	0·00777	0·00677	0·00781
1·6221	0·03602	0·016179	0·03371	0·01400	0·01177	0·01418
1·9007	0·04826	0·021315	0·04467	0·01880	0·01540	0·01896

x	H_a	H_1	H_2
0·926	1·800	2·1282	2·1282
1·0763	2·333	1·3605	2·538
1·2506	2·340	1·3627	2·445
1·6221	2·572	1·3751	2·378
1·9007	2·566	1·3843	2·356
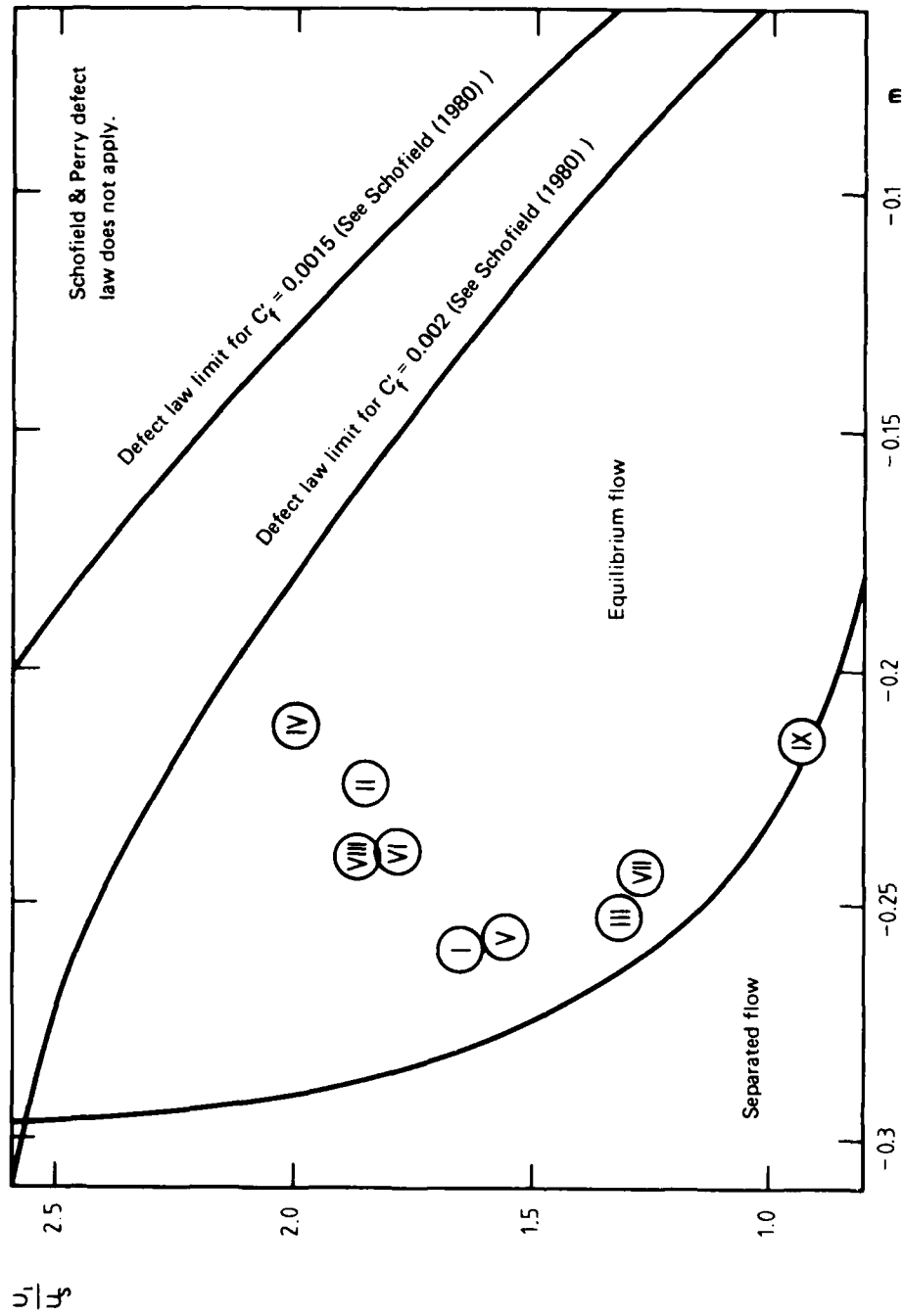
Numerals in circles give the equilibrium layer number. The equilibrium layers are defined in Table 1.

FIG. 1. LIMITS FOR EQUILIBRIUM FLOW.
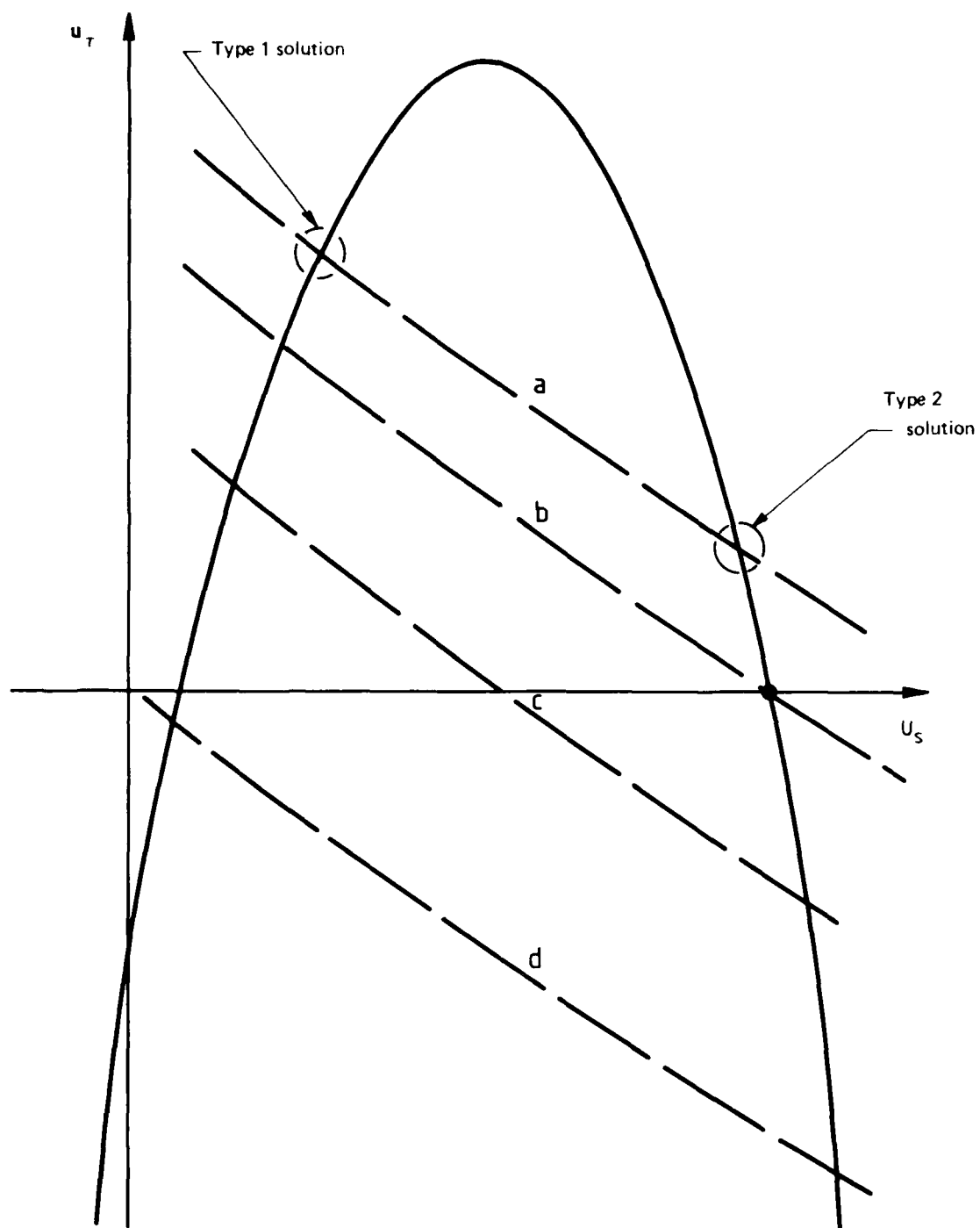
FIG. 2. SOLUTION CURVES
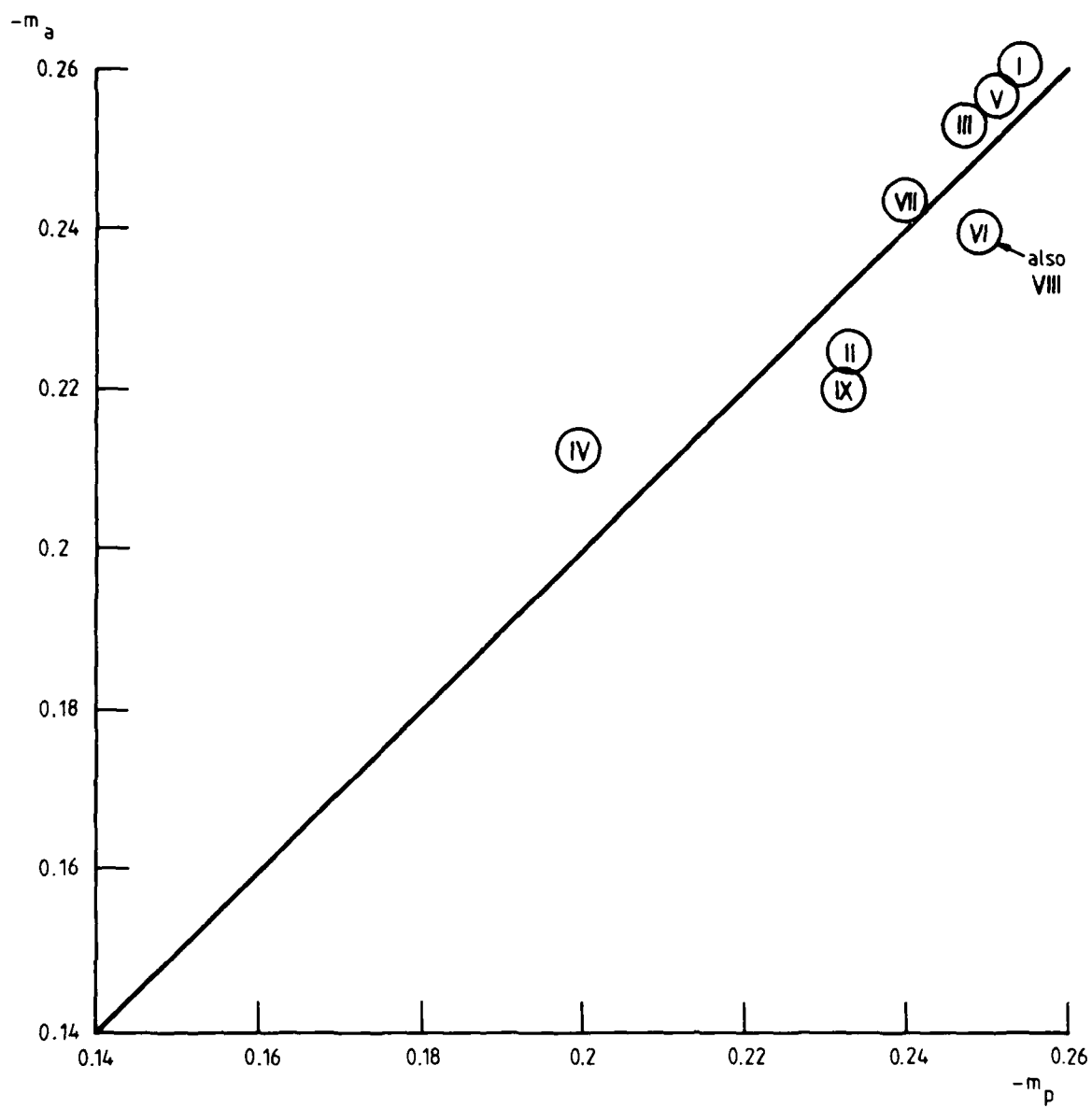
FIG. 3a. PREDICTED AND ACTUAL VALUES OF THE FREE STREAM VELOCITY
EXPONENT (m).
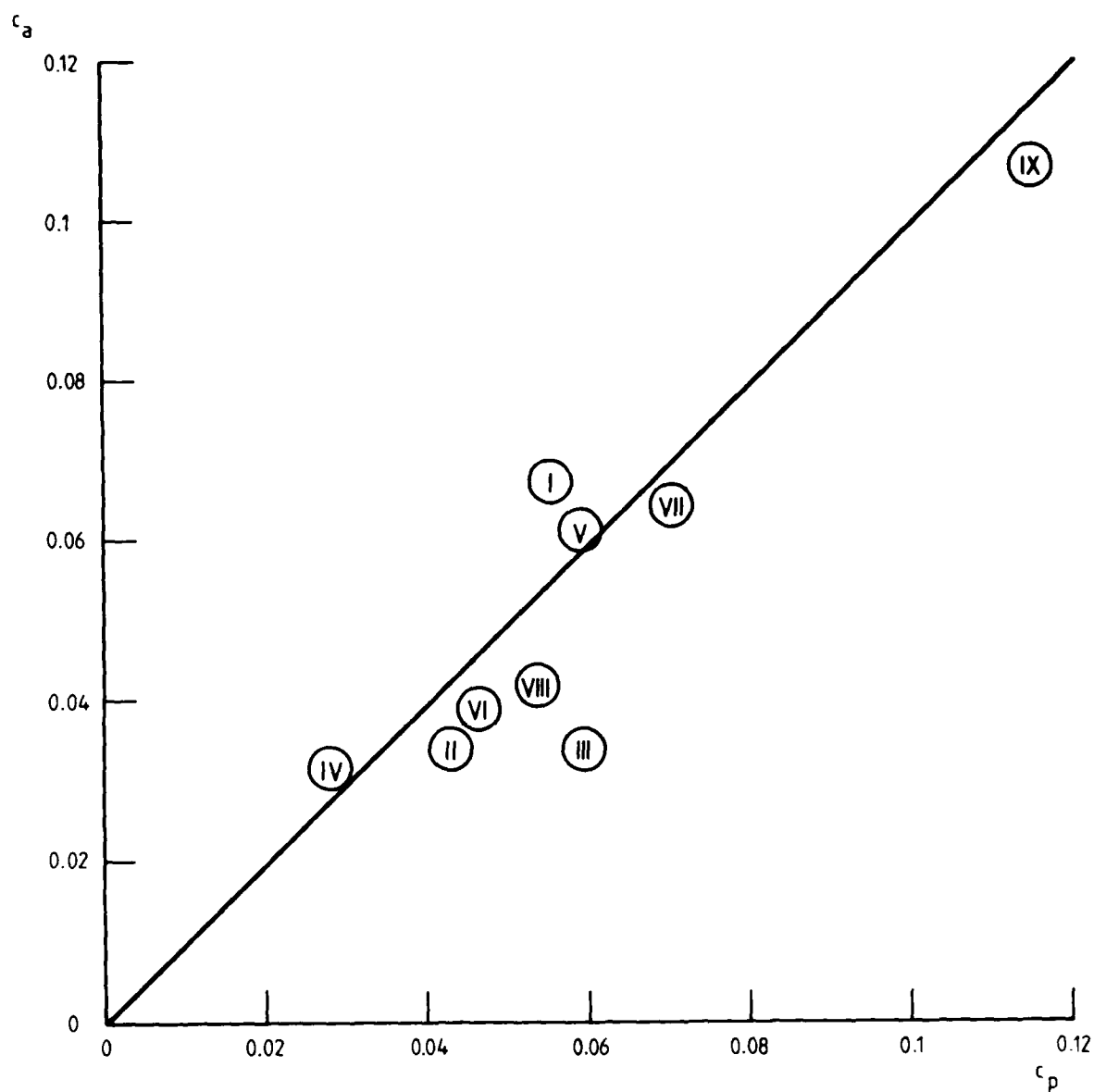
, line of perfect agreement.

FIG. 3b. PREDICTED AND ACTUAL VALUES OF BOUNDARY LAYER GROWTH RATE (c).
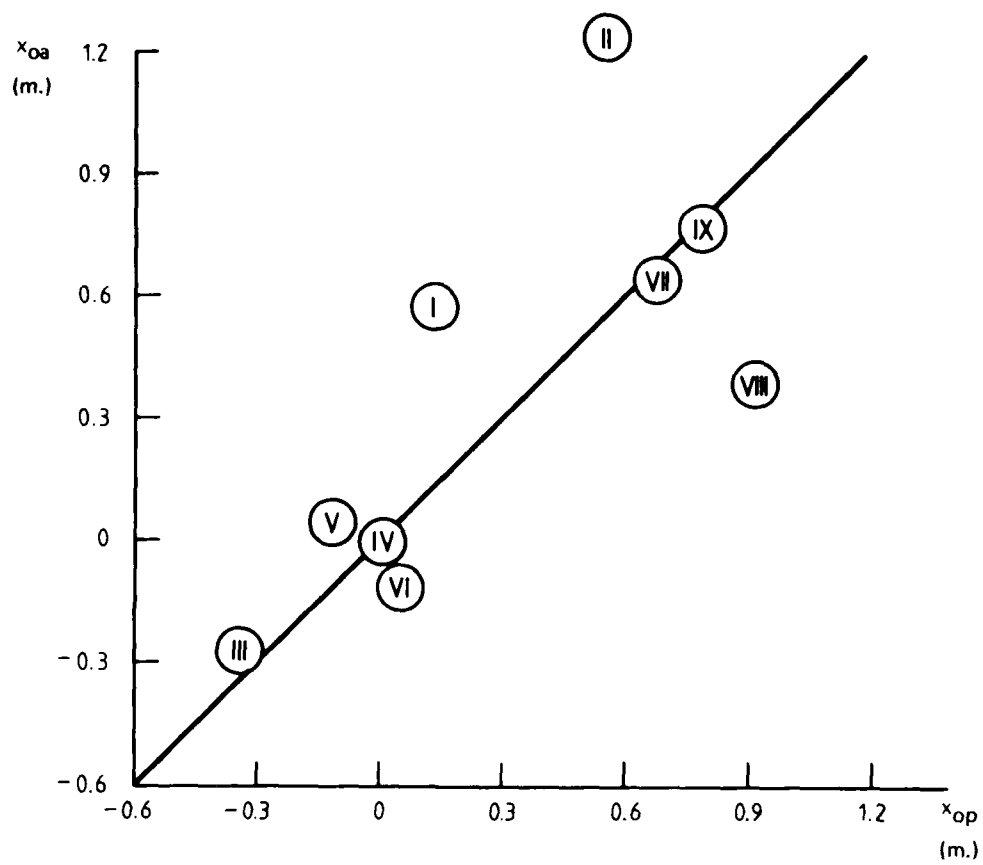
———, line of perfect agreement.

FIG. 3c. PREDICTED AND ACTUAL VALUES OF EFFECTIVE ORIGIN OF THE LAYERS.
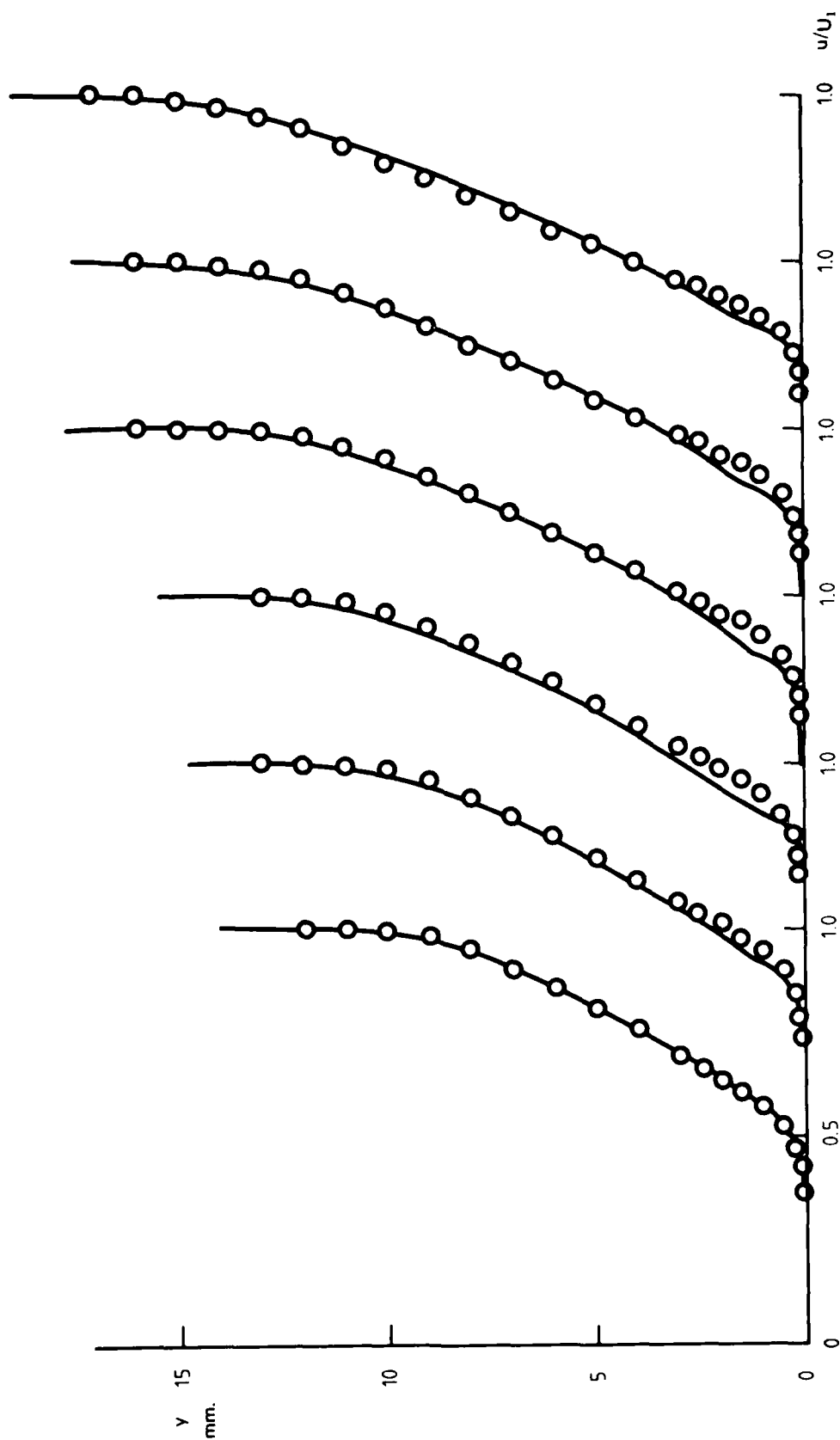
——— , predicted; O, actual values.

FIG. 4. PREDICTED AND ACTUAL MEAN VELOCITY PROFILES. LAYER I
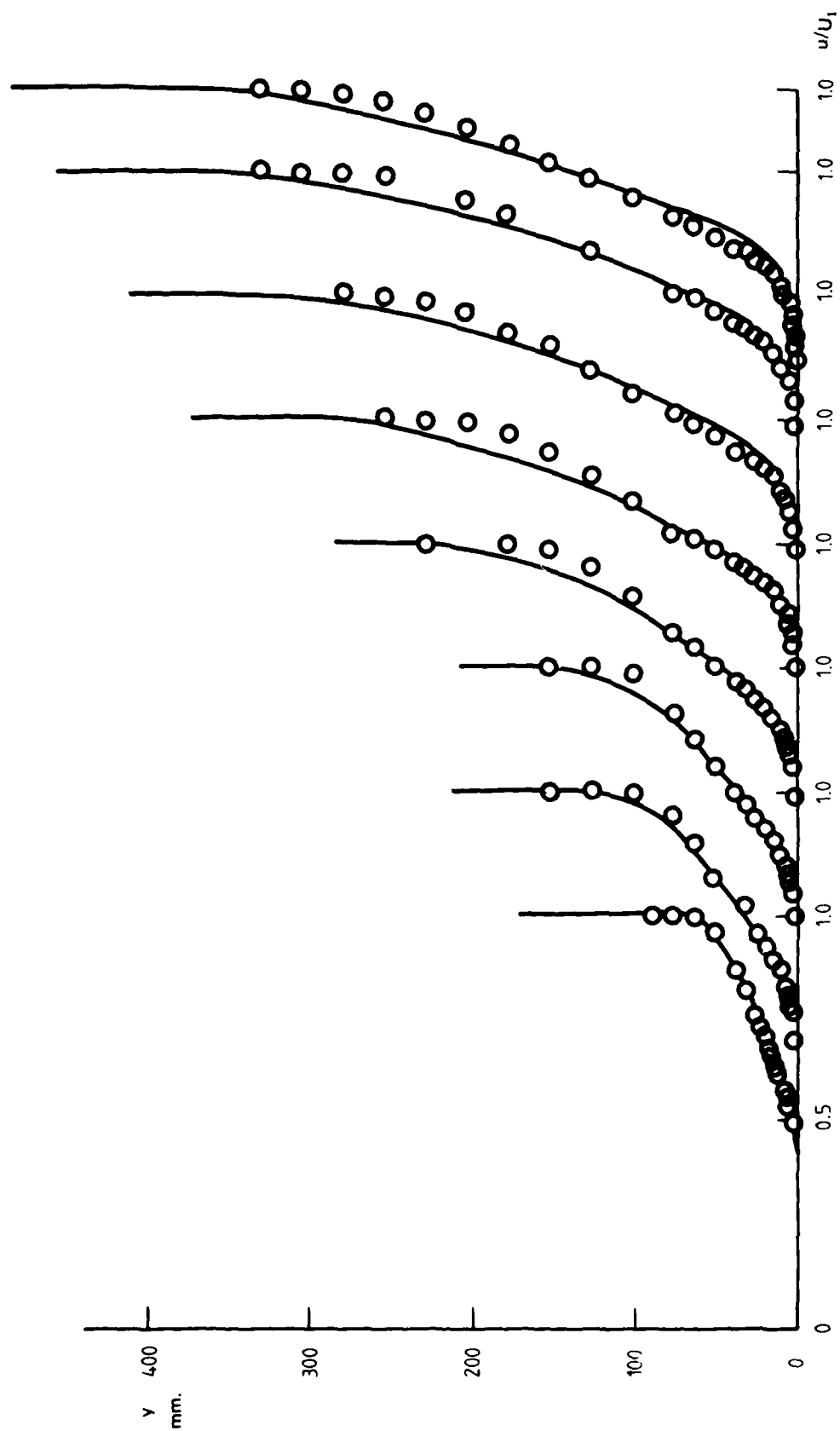
————, predicted; O, actual values.

FIG. 4. CONTINUED. LAYER II

——— , predicted; O , actual.
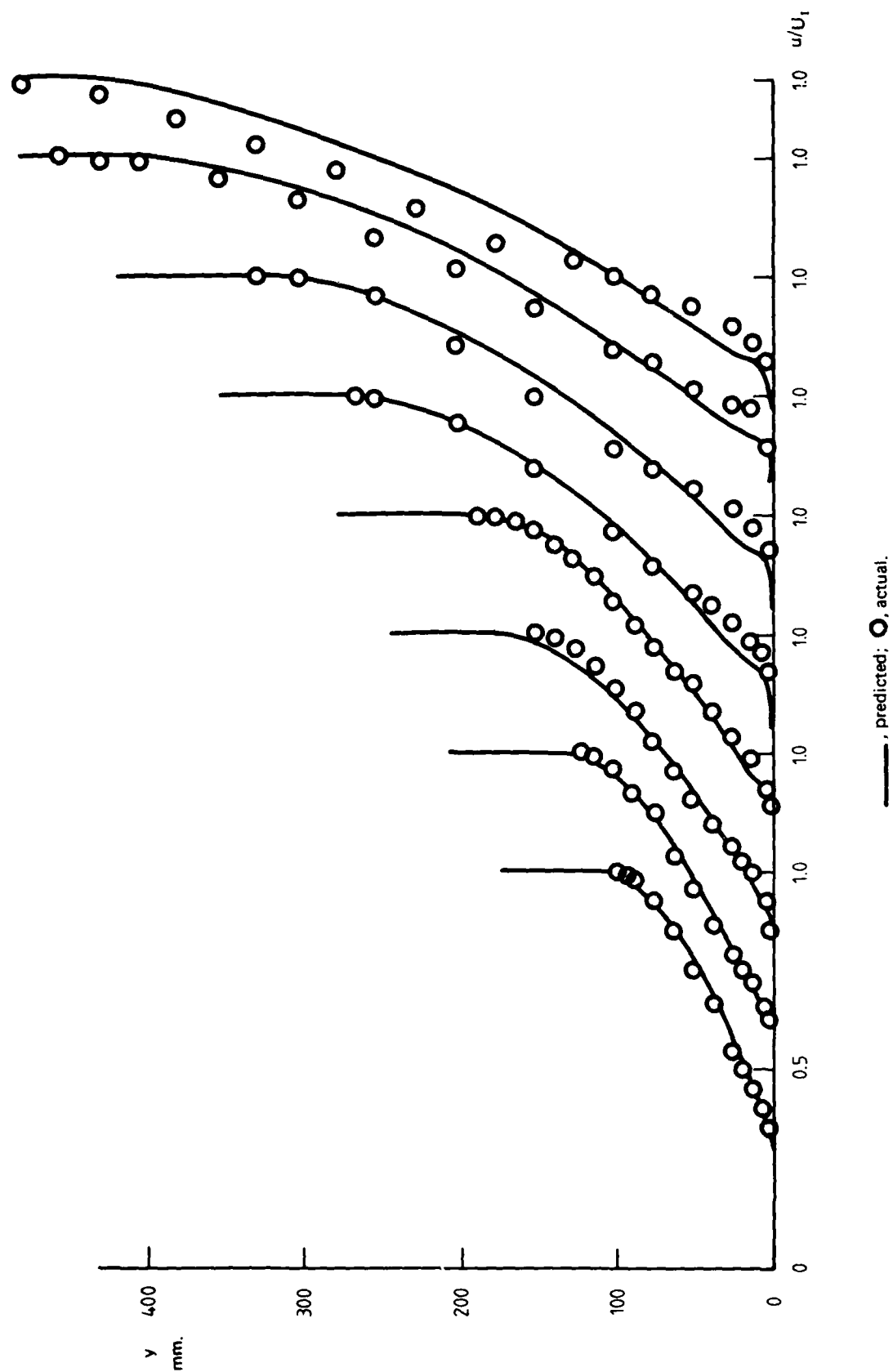
FIG. 4. CONTINUED. LAYER III
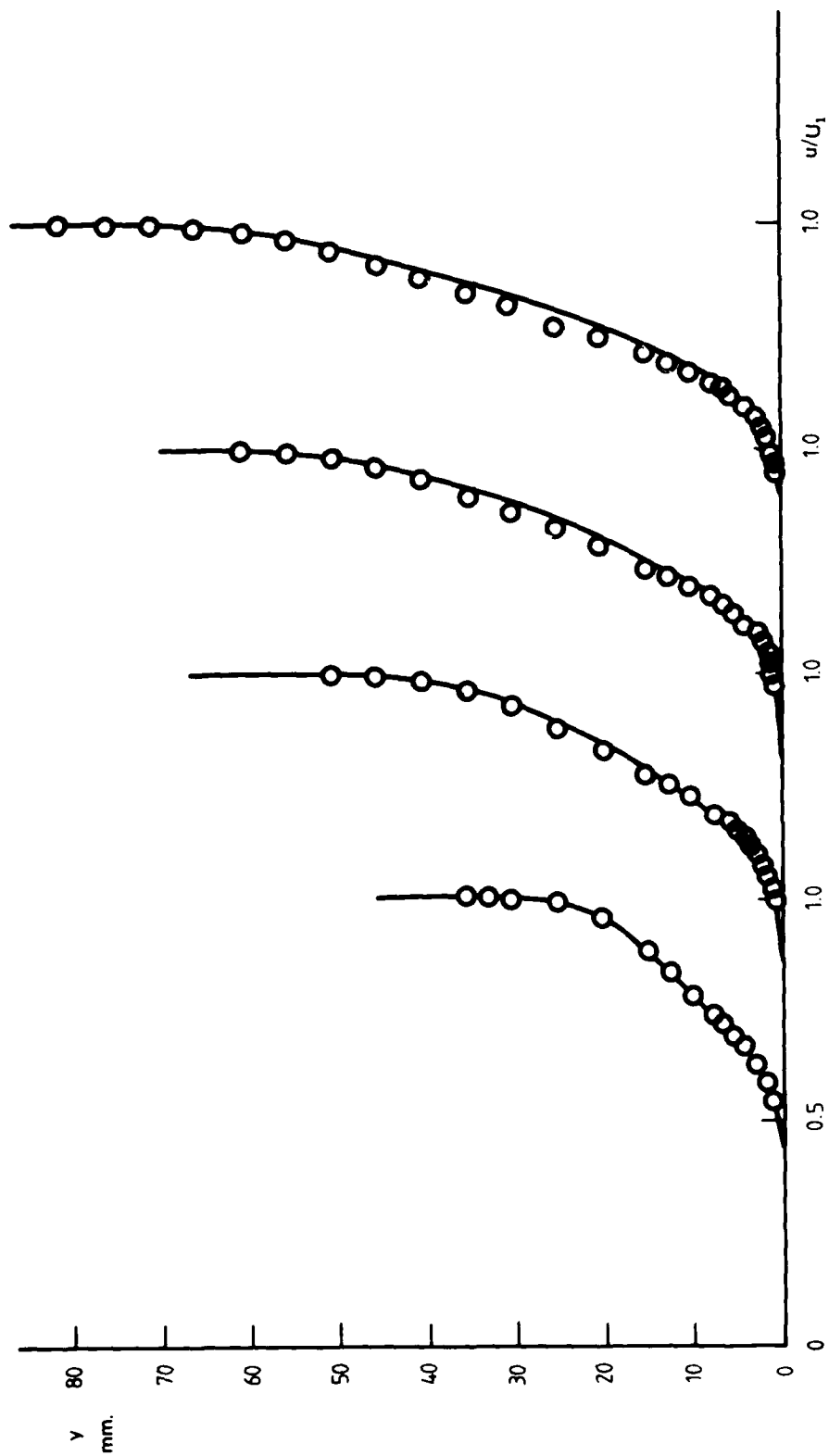
————, predicted; O, actual.

FIG. 4. CONTINUED. LAYER IV

FIG. 4. CONTINUED. LAYER V
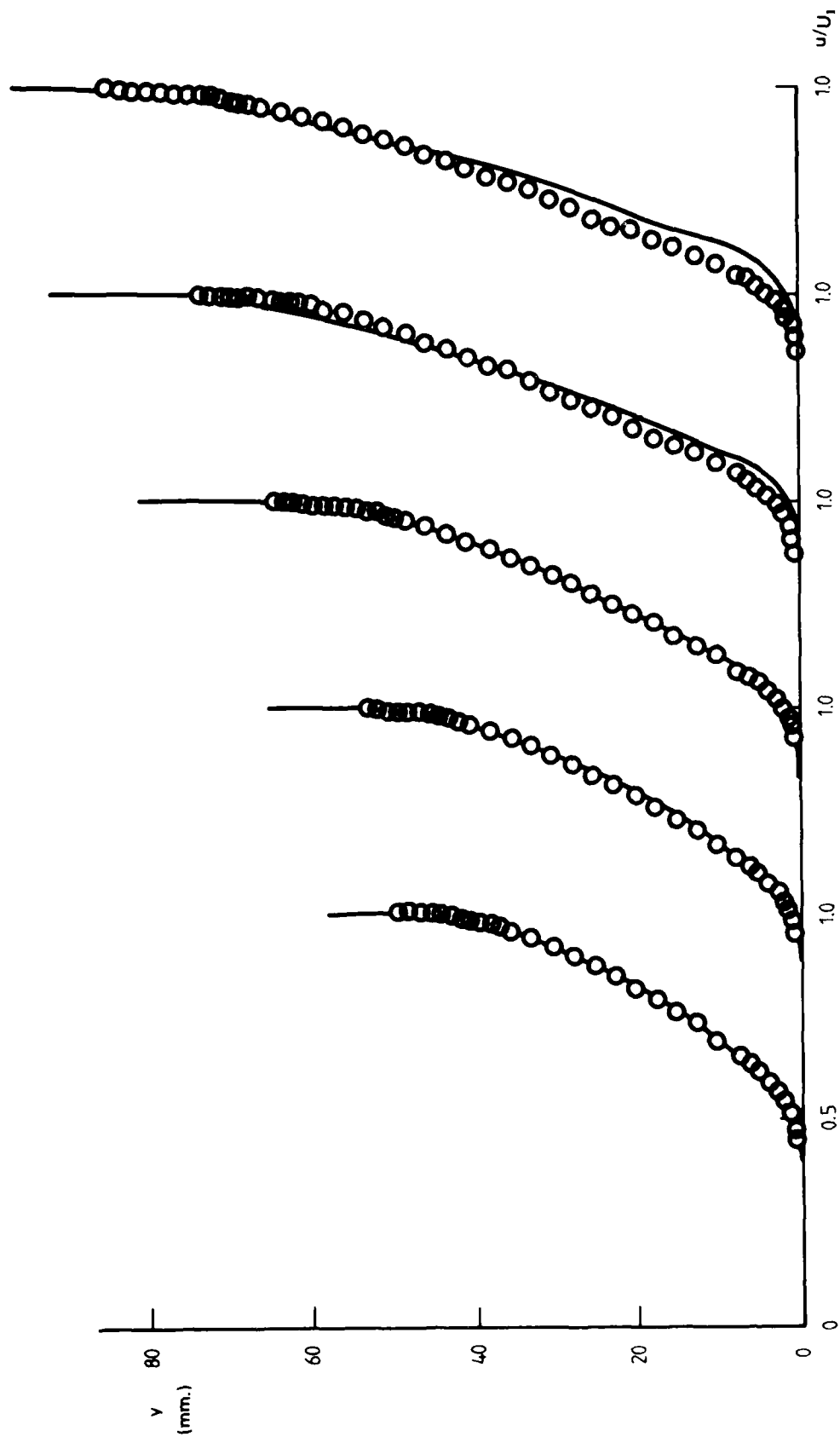
——, predicted; O, actual.

y
mm.

u/U₁

, predicted; O, actual.

FIG. 4. CONTINUED. LAYER VI

———, predicted: O, actual.

FIG. 4. CONTINUED. LAYER VII

———, predicted; O, actual.
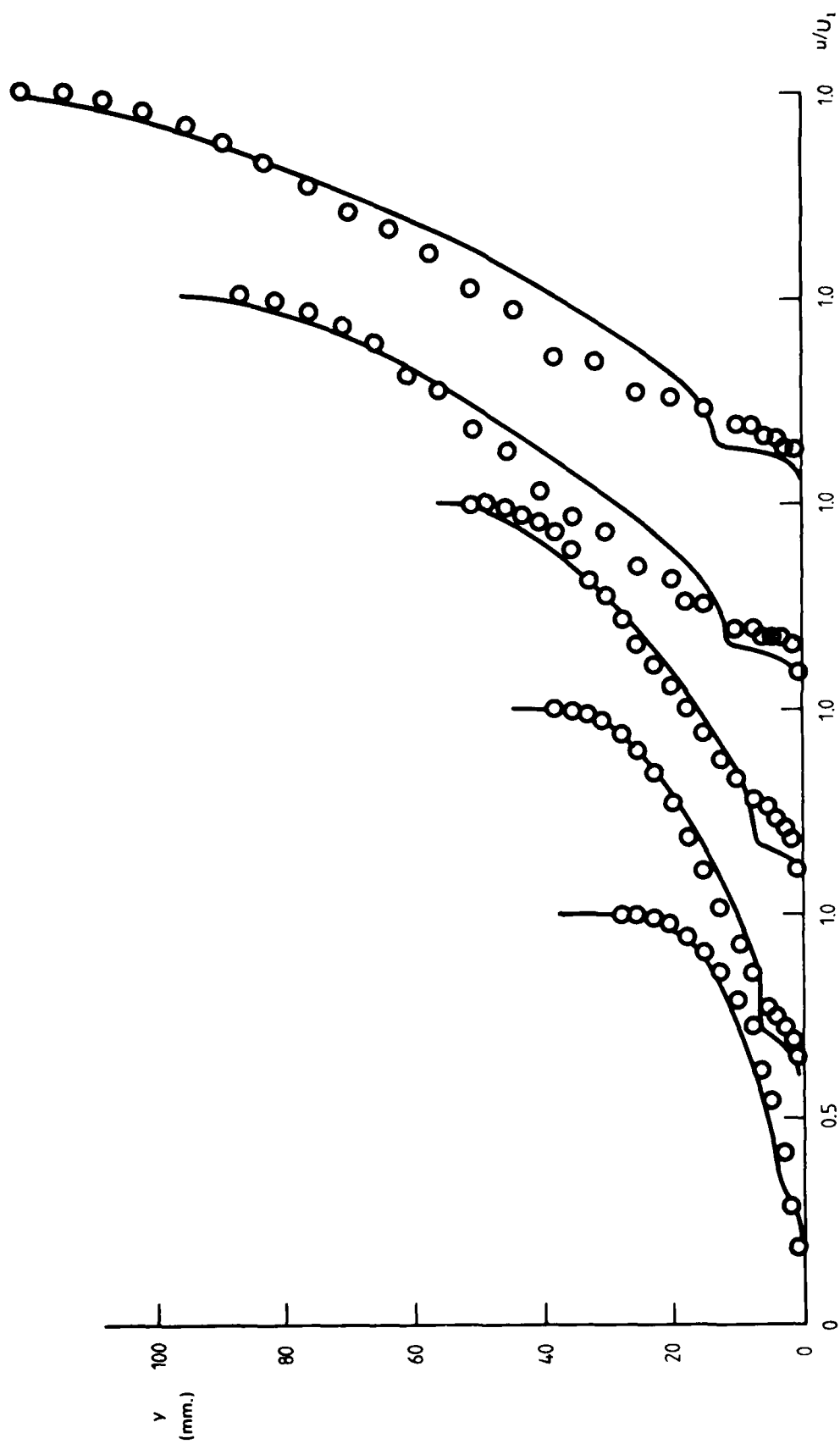
FIG. 4. CONTINUED. LAYER VIII

FIG. 4. CONCLUDED. LAYER IX
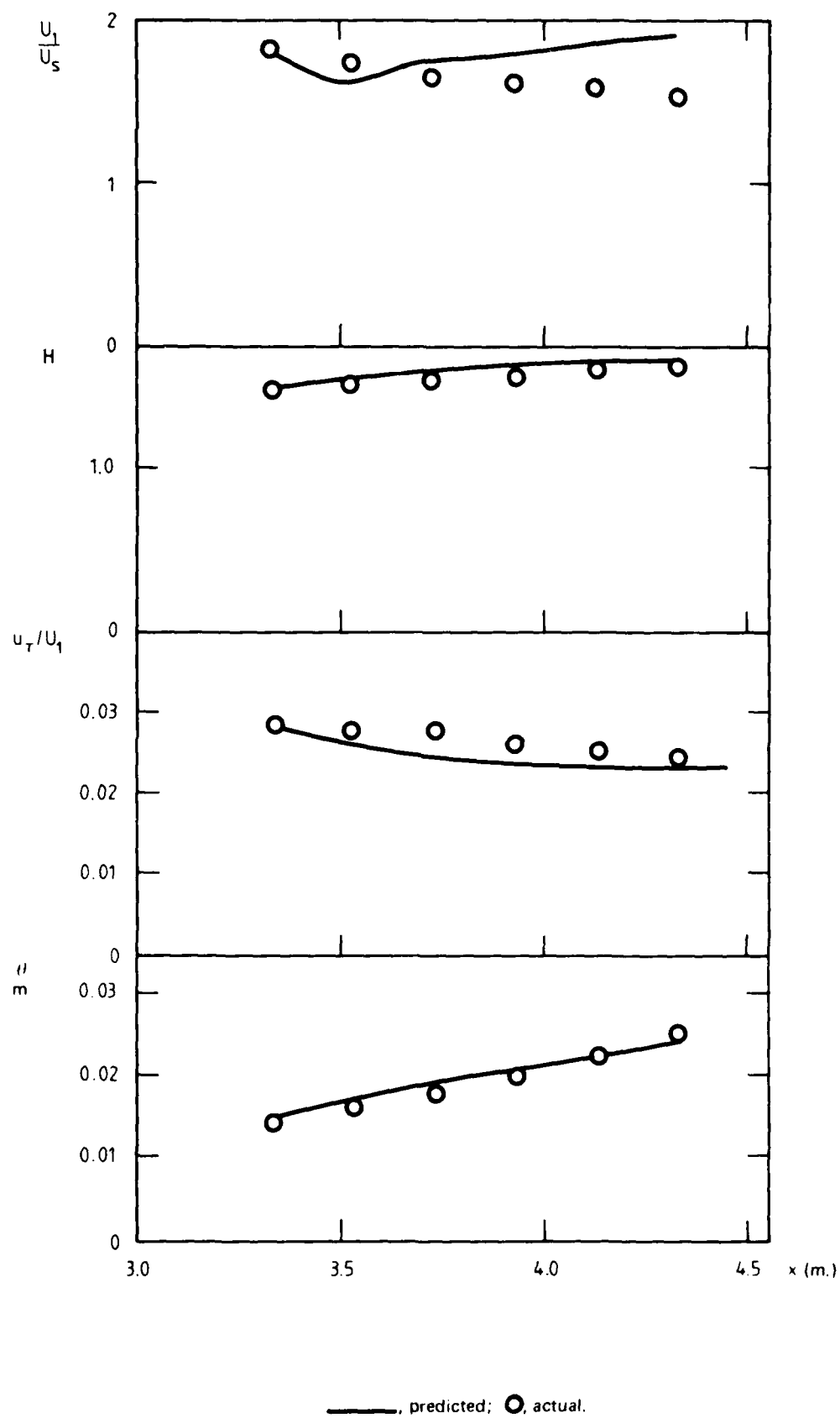
———, predicted; O, actual.

FIG. 5. COMPARISON OF PREDICTED AND ACTUAL FLOW PARAMETERS. LAYER I.
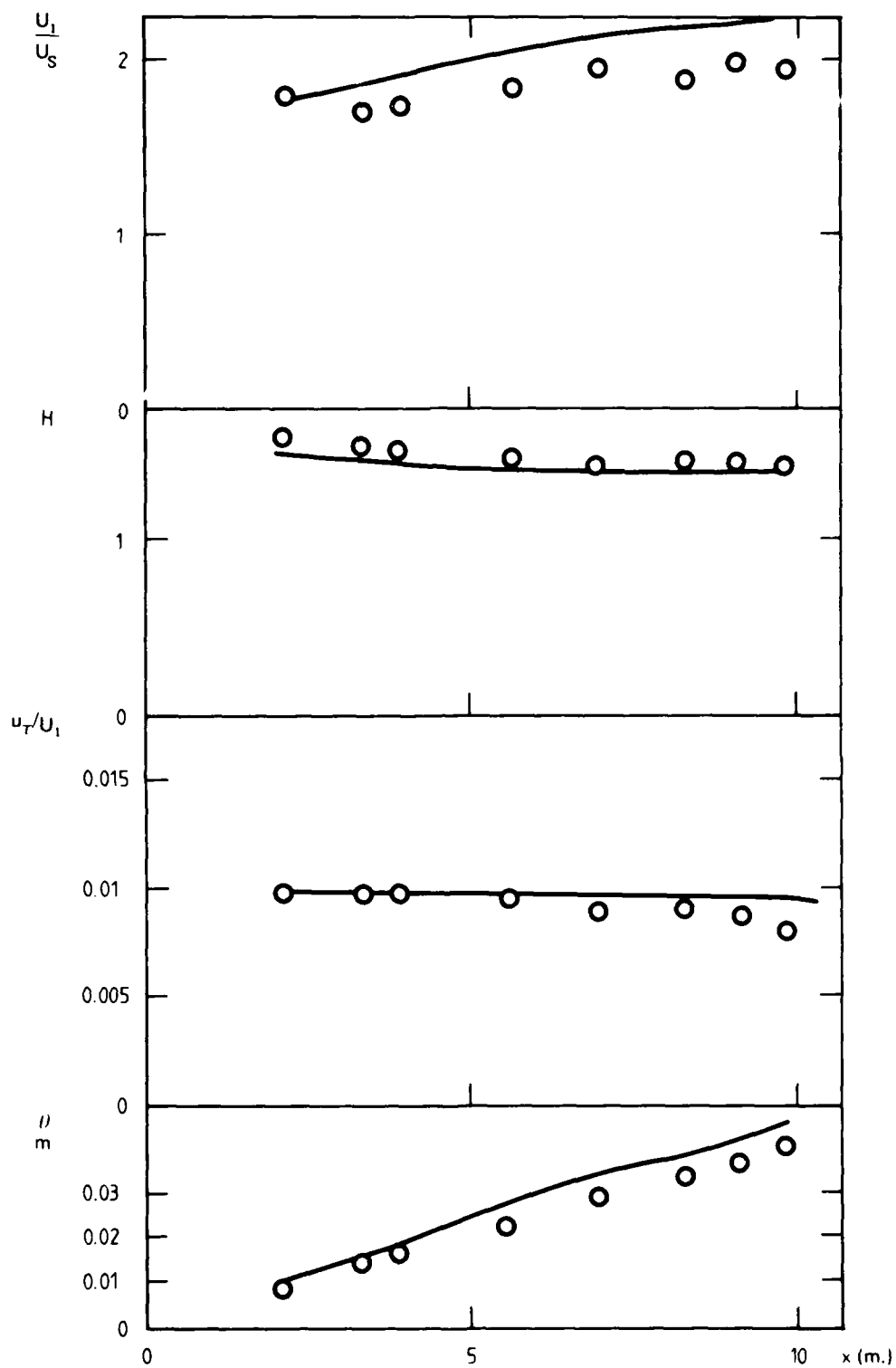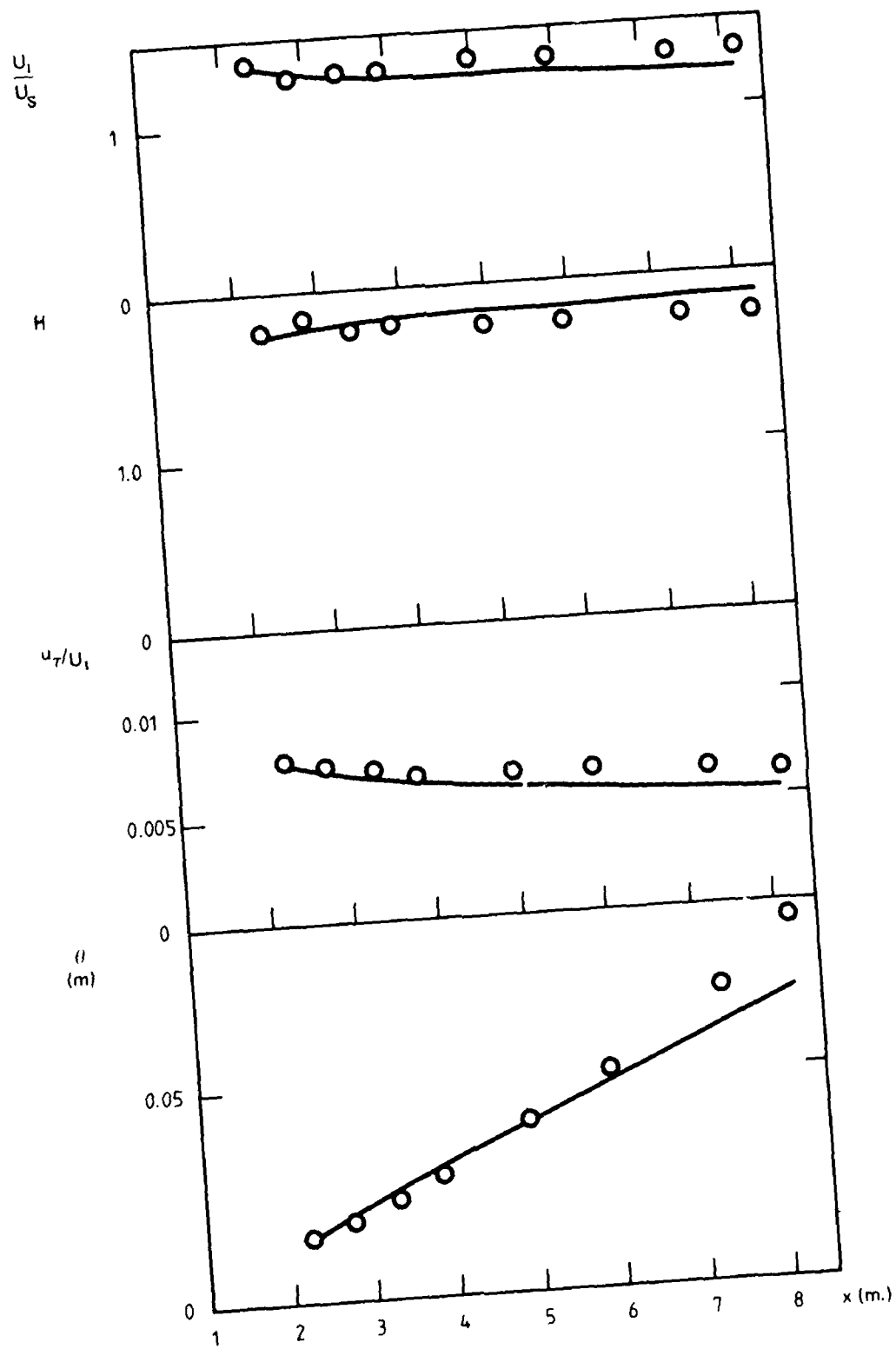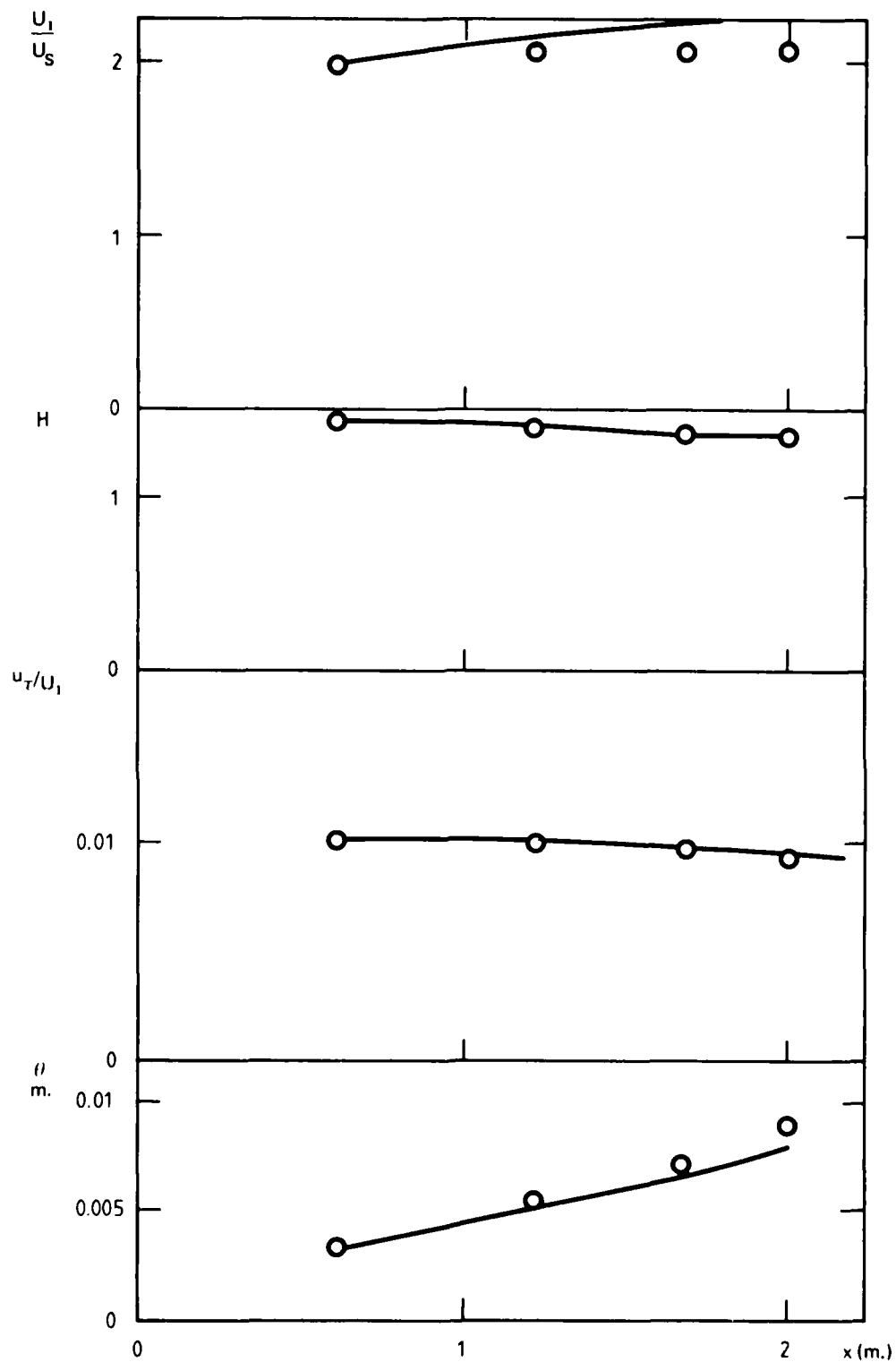
—— , predicted; O , actual.

FIG. 5. CONTINUED. LAYER II

———, predicted; O, actual.

FIG. 5. CONTINUED. LAYER III

, predicted; O, actual.

FIG. 5. CONTINUED. LAYER IV

, predicted; O, actual.

FIG. 5. CONTINUED. LAYER V
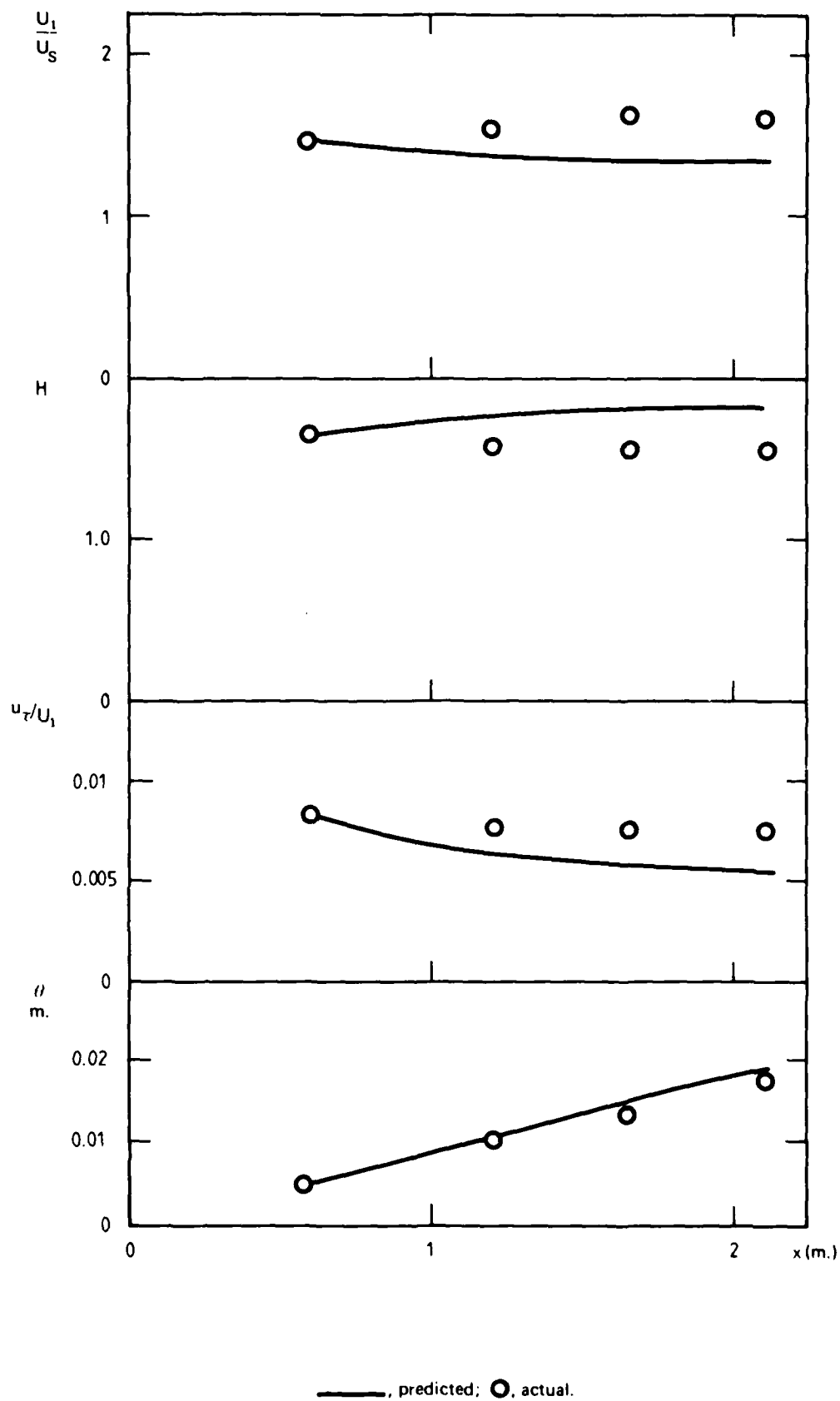
—— , predicted; O, actual.
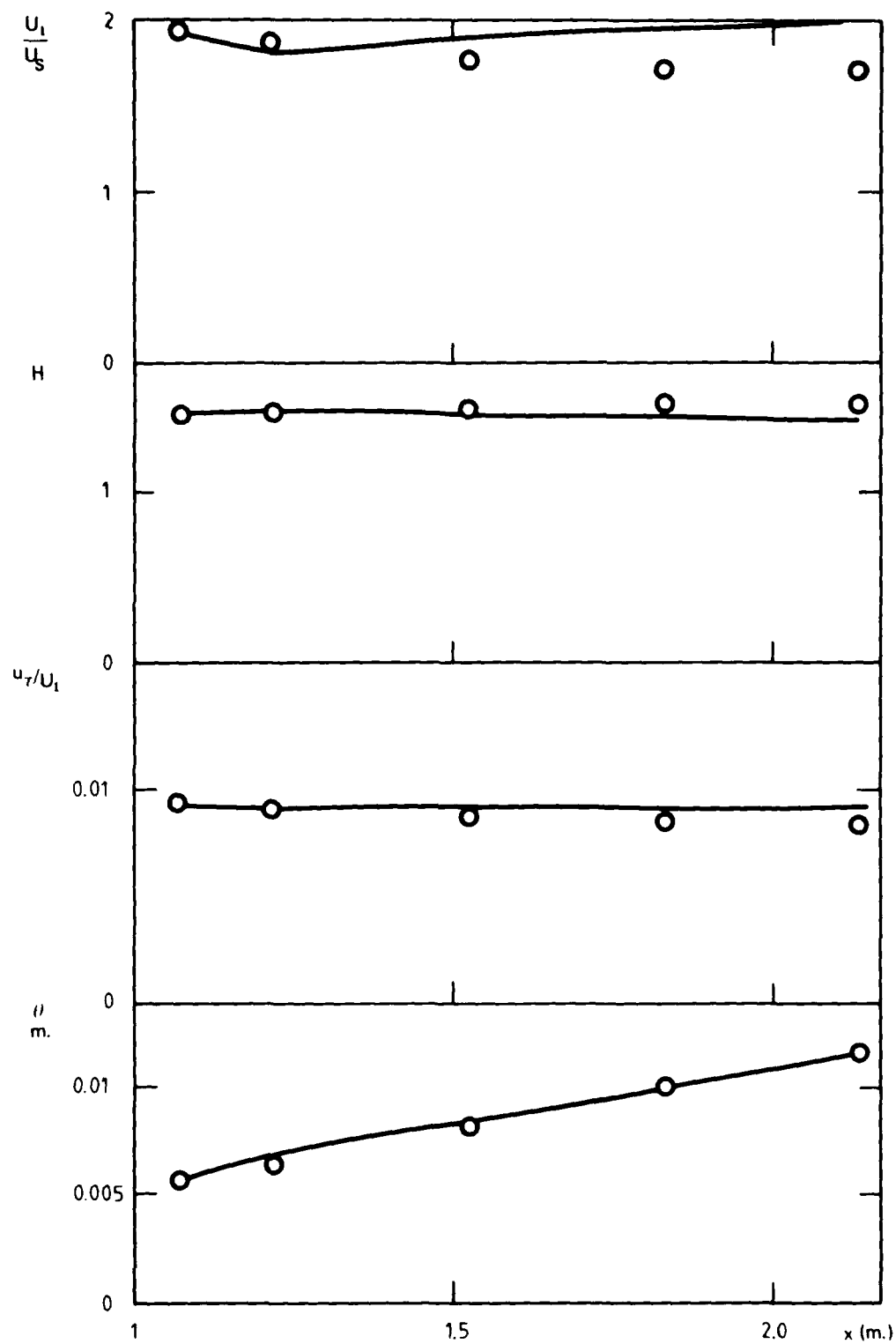
FIG. 5. CONTINUED. LAYER VI

———, predicted; O, actual.
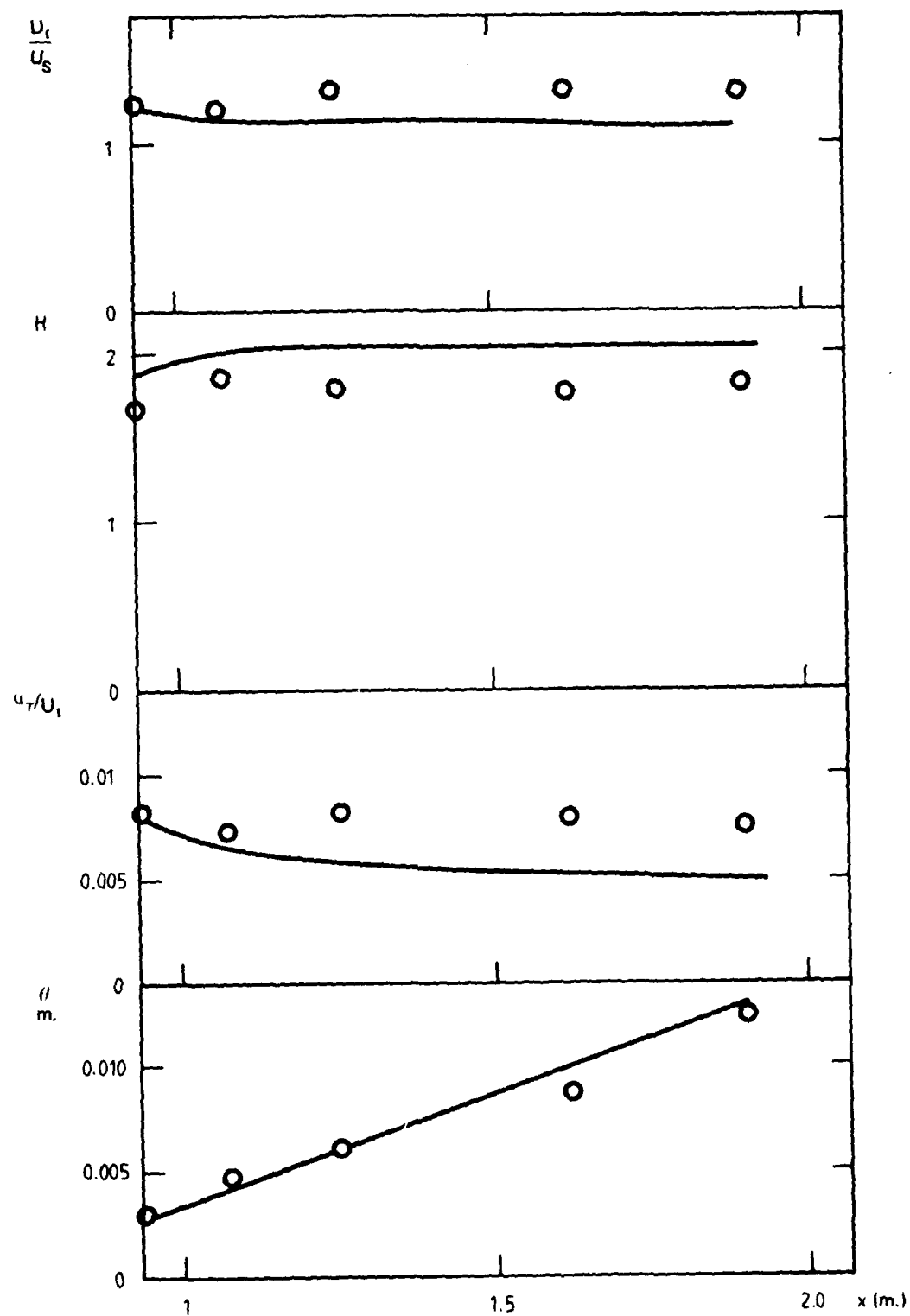
FIG. 5. CONTINUED. LAYER VII
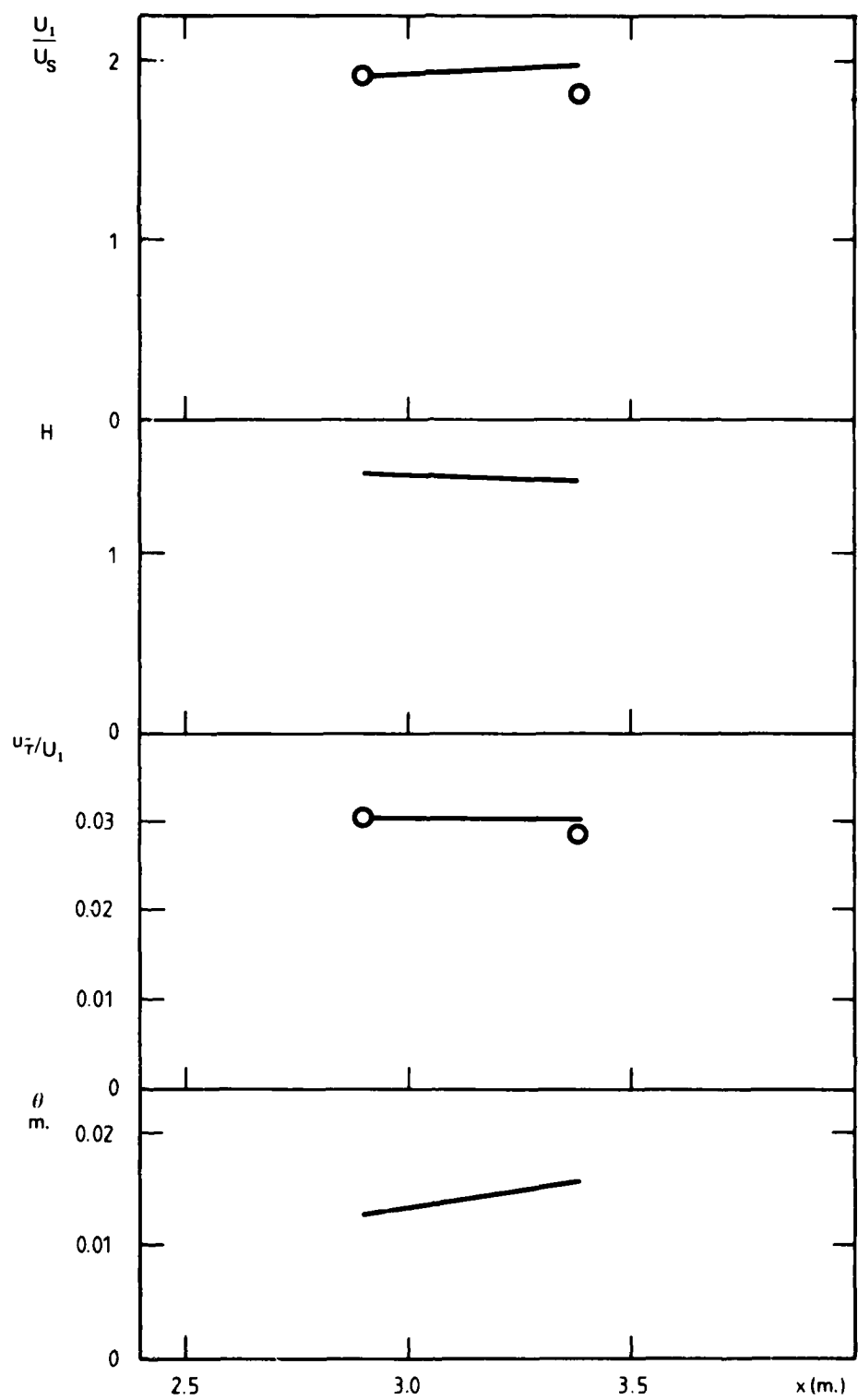
_____ , predicted; O, actual.

FIG. 5. CONTINUED. LAYER VIII
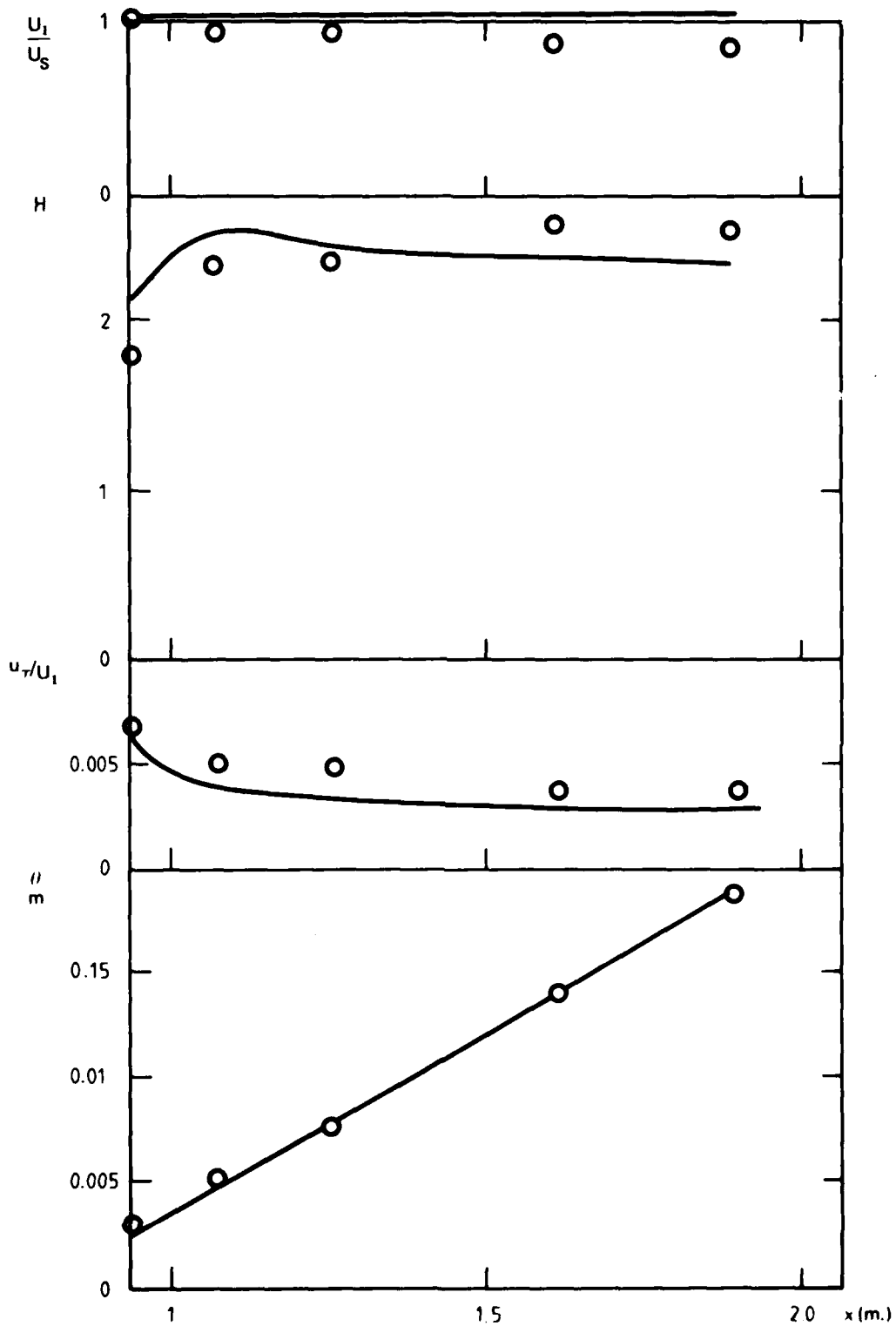
_____ , predicted; O, actual.

FIG. 5. CONCLUDED. LAYER IX

$$\frac{\tau(\eta)}{\frac{1}{2}\rho U_1^2} \times 10^3$$

———— , predicted profile using predicted parameters;

– – – , " " " actual " " ;

⊙ , experimental points.
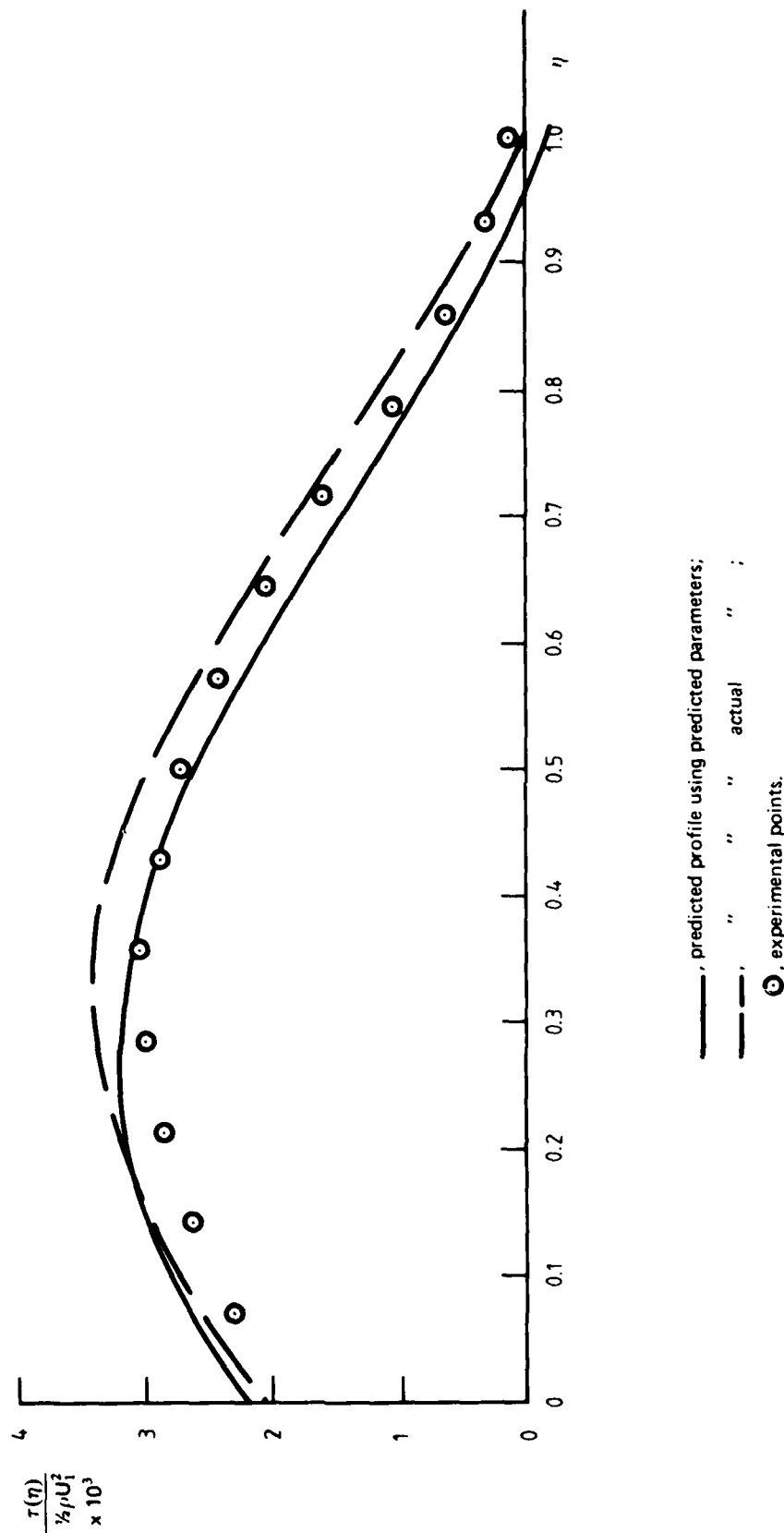
FIG. 6. SHEAR STRESS PROFILES. LAYER IV
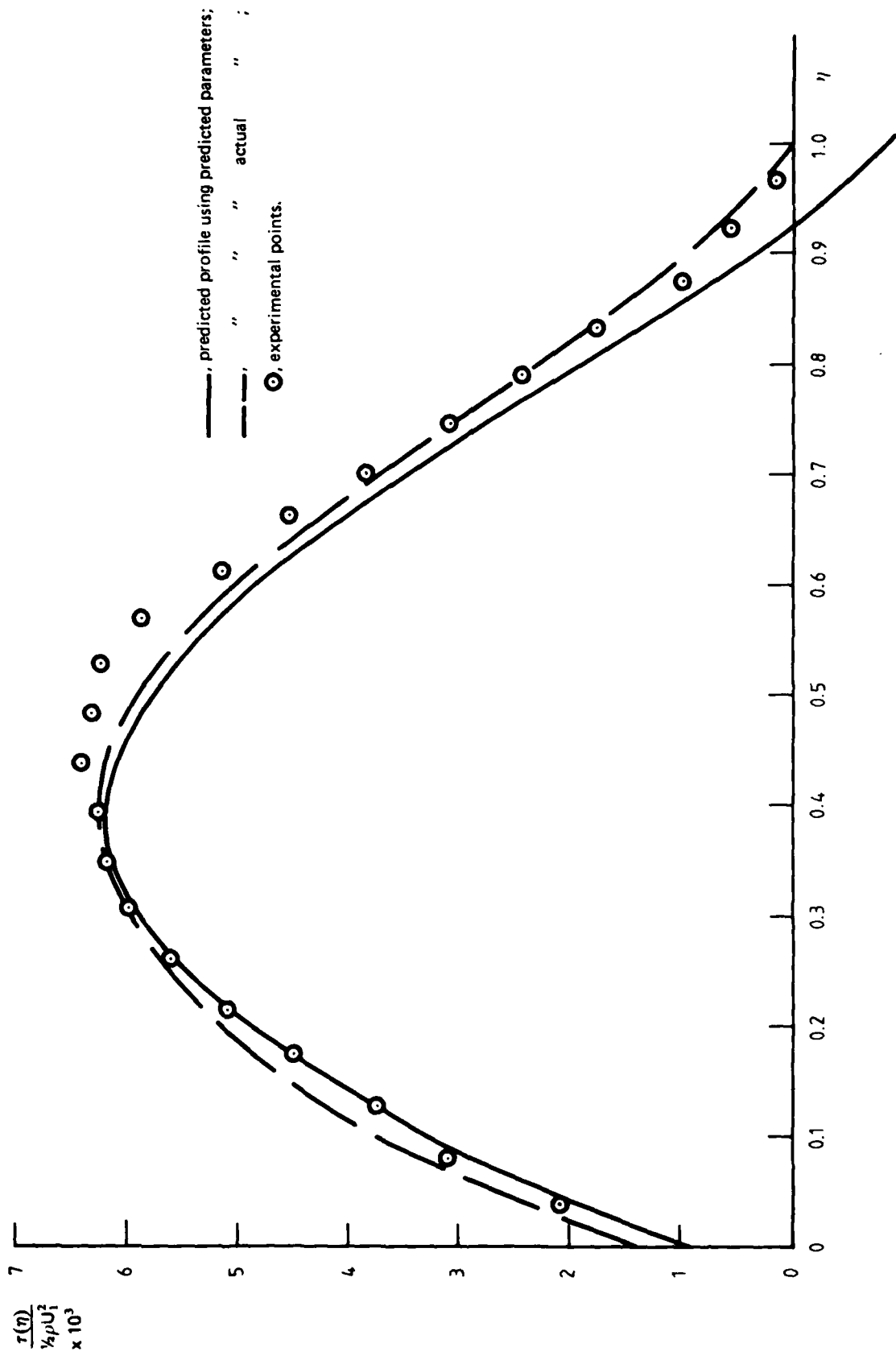
FIG. 6. CONTINUED. LAYER V
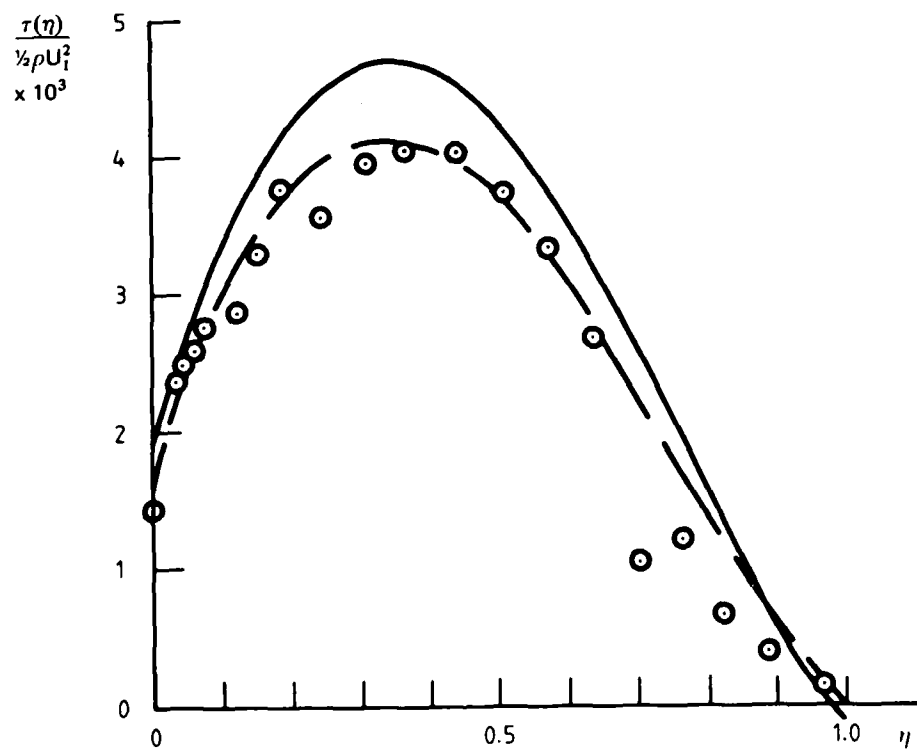
predicted profile using predicted parameters;

" " " actual " ;

⊙, experimental points.

$\dfrac{\tau(\eta)}{\frac{1}{2}\rho U_1^2} \times 10^3$

η

FIG. 6. CONCLUDED. LAYER VI

$\dfrac{\tau(\eta)}{\frac{1}{2}\rho U_i^2} \times 10^3$

————, predicted profile using predicted parameters;

— — —, "   " "   actual   "   ;

○, experimental points.

FIG. 6. CONTINUED. LAYER VIII

Numerals in circles denote the measured equilibrium layers;
numerals in squares denote predicted equilibrium layers;
numerals in triangles denote the alternative equilibrium layers yielded by the method.
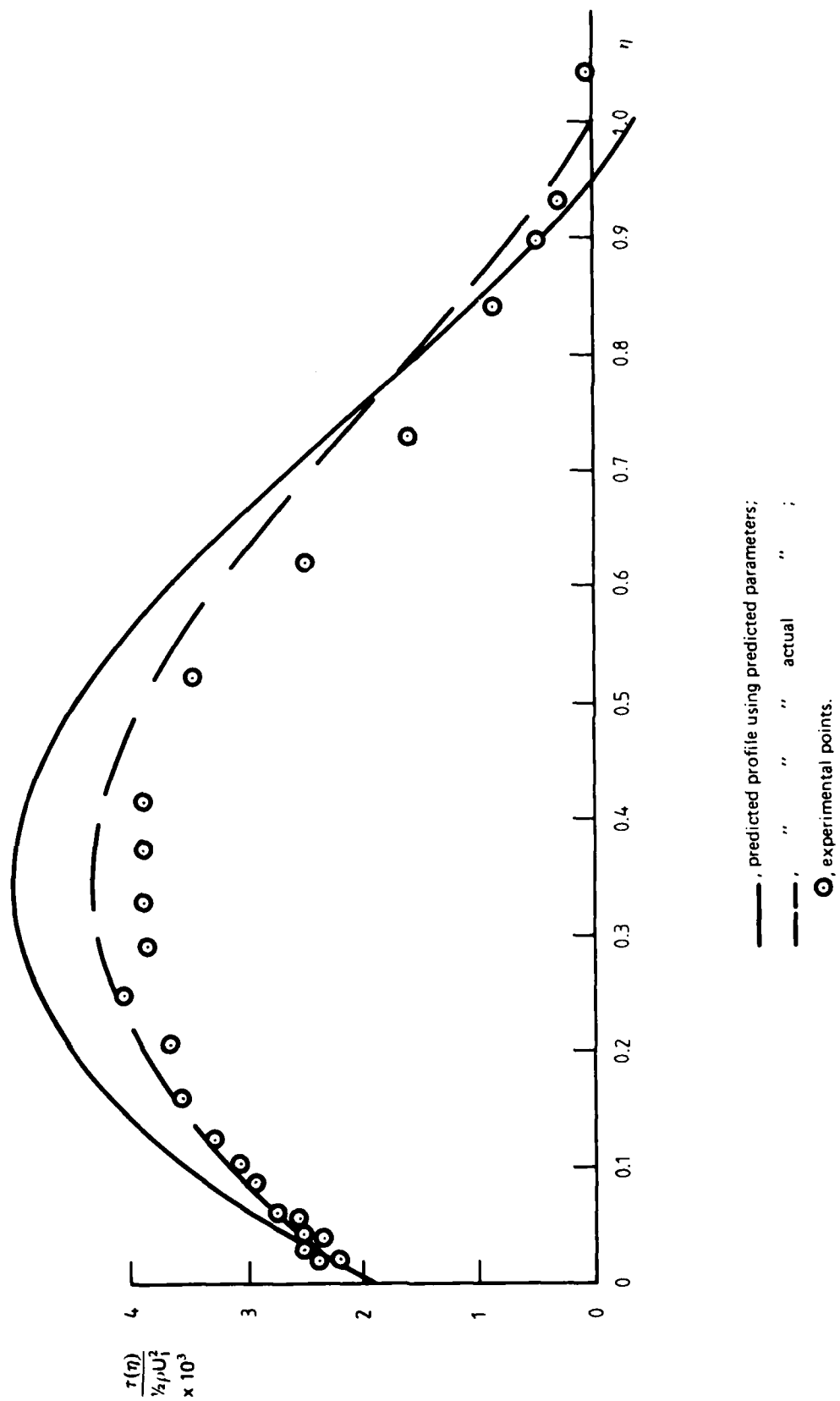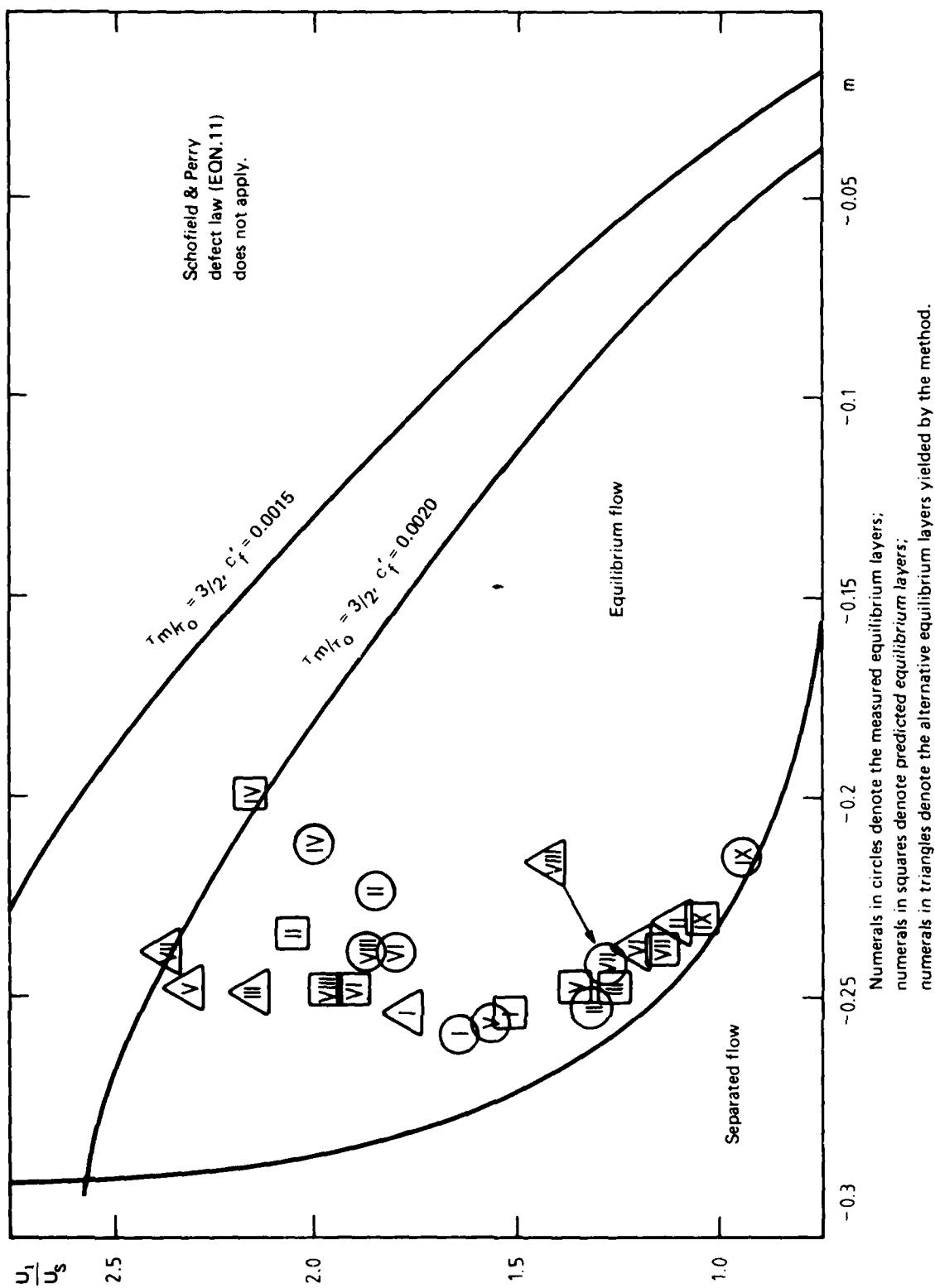
FIG. 7. PREDICTED EQUILIBRIUM LAYERS

DISTRIBUTION

Copy No.

D

FI